

Nihan Atak, BSc

**Designing and testing a microfluidic device to investigate
chemotactic behavior of sperm cells**

MASTER'S THESIS

to achieve the university degree of

Master of Science

Master's degree program: Chemical and Pharmaceutical Engineering

submitted to

Graz University of Technology

Supervisors

Segerink, Loes I., Assoc.Prof.

Department of Biomedical and Environmental Sensor systems
BIOS Lab-on-a-chip Group, University of Twente, Enschede, the Netherlands

Mayr, Torsten, Assoc.Prof. Dipl.-Chem.

Institute of Analytical Chemistry and Food Chemistry, TU Graz

Graz, August 2020

ABSTRACT

Screening and investigating sperm cells behavior is important for human fertility studies. In mammals' body, it was reported that chemotaxis is one of the main factors that affects sperm cells behavior. Therefore, we developed a microfluidic device to observe the sperm chemotactic behavior while considering effect of temperature. To produce microfluidic chips, mixture of gelatin and agarose (8:1 w:w) was used. Gelatin and agarose were dissolved in PBS separately at 60 °C and 80 °C respectively and mixed. The mixture, then, was poured into polydimethylsiloxane (PDMS) mold. Afterwards, hydrogel chips were bonded to glass slide covalently which creates free chemical ends on the glass surface to allow bonding. For that purpose, (3-Aminopropyl)triethoxysilane (APTES) (3 v/v %, in deionized (DI) water) and glutaraldehyde (10 v/v %, in PBS) solutions were prepared. Hydrogel chips were bonded with glass slide. After bonding, fluorescein sodium salt solution (0,005%) was used due to its molecular weight is approximately same as progesterone to create a gradient. According to results of fluorescein trials, gradient formation time was optimized and used in chemotaxis experiments. 1 μM concentration of progesterone solution was used. After creating chemoattractant gradient, sperm cells injected into the device and observed. It was found that spermatozoa have chemotaxis behavior towards to progesterone.

AFFIDAVIT

I declare that I have authored this thesis independently, that I have not used other than the declared sources/resources, and that I have explicitly indicated all material which has been quoted either literally or by content from the sources used. The text document uploaded to TUGRAZonline is identical to the present master's thesis.

Date

Signature

ACKNOWLEDGEMENT

I would like to express my deepest appreciation to my supervisors Loes I. Segerink and Jorien Berendsen in University of Twente and Torsten Mayr in University of Technology Graz who provided me the possibility to complete this thesis. A special thanks goes to Josh T. Loessberg-Zahl who helped me with the bonding procedure and Martijn Tibbe for his precious support. Additionally, I want to thank to all BIOS Lab-on-a-chip members for their contributions.

A very special gratitude goes out to Erasmus+ for providing the funding for me to do my research abroad.

Furthermore, I am grateful to my mother Semra Atak, my father Mehmet Atak, my siblings Dihan Atak and Ufuk Atak who have provided me with unfailing support and continuous encouragement.

TABLE OF CONTENTS

ABSTRACT	i
AFFIDAVIT	ii
ACKNOWLEDGEMENT	iii
1. INTRODUCTION	1
1.1 Microfluidic Devices and Their Roles in Pharmaceutical Applications	1
1.2 Chemotaxis.....	3
1.3 Hydrogels	4
1.3.1 Properties of Hydrogels	5
1.3.2 Gelatin and Agarose.....	6
2. THEORETICAL BACKGROUND	7
3. METHODOLOGY	9
3.1 Instrumentation.....	9
3.1.1 Oxygen Plasma Cleaner	9
3.1.2 Microscopes	9
3.1.3 Hot plate.....	11
3.1.4 Punches	12
3.2 Method	13
3.2.1 PDMS Mold Fabrication.....	13
3.2.2 Hydrogel Solution Preparation	14
3.2.3 Hydrogel Chip Fabrication and Bonding.....	15
3.2.4 Cell Viability Experiments	17
3.2.5 Gradient Trials	18
3.2.6 Progesterone Experiments	19
3.2.7 Statistical Analysis.....	23

4. RESULTS AND DISCUSSION	24
4.1 Optimization of Hydrogel Preparation.....	24
4.2 Viability.....	24
4.3 Optimization of Gradient Formation Time	30
4.4 Progesterone Experiments.....	35
5. CONCLUSION AND OUTLOOK.....	41
6. LIST OF FIGURES	42
7. APPENDIX.....	44
8. REFERENCES.....	45

1. INTRODUCTION

1.1 Microfluidic Devices and Their Roles in Pharmaceutical Applications

Microfluidic devices are the microscale devices that allow make some experiments with very small volumes of fluids in a micron sized channel or chambers. This technology has started to develop in 1980s and basically consists of fabrication of the device with channels and control the flow of small amount of fluids. Microfluidics or lab-on-a-chip technology is a multidisciplinary field that combines nanotechnology, biotechnology, biochemistry, physics and engineering [1]. They have been used for several purposes such as drug screening, biological assays and sperm chemotaxis as well as for other sperm experiments, for instance, sperm-sorting in a lab-on-a-chip device in parallel [2]. Reasons that microfluidics were preferred are easily mimicking the environment, controlling the parameters, rapid production methods with smaller sample volumes, enabling more accurate conditions for 3D cell-culture, allowing rapid heat and mass transfer [1, 3, 4].

Several system components can be used to produce a microfluidic device, for example, pumps, valves, mixers, heaters and those increase the rate of efficiency in comparison with conventional macrosystems [5]. During fabrication, material types, compatibility of these materials, properties of the device such as number of inlet/outlets are the parameters that taken into account. Often these devices are made of polydimethylsiloxane (PDMS) or polymethylmethacrylate (PMMA) because these polymers are easy to use, cheap and biologically inert, yet they can be deformed with strong solvent exposure [1].

In pharmaceutical engineering, one of the main aims is reduction of the production costs and duration of pharmaceuticals production [2, 6]. Mostly the macroscopic systems are in use during drug discovery process, since it's a must to provide a throughput, however it has disadvantages such as expensive and long processes [5]. As a novel solution microfluidics can be used in drug discovery, preclinical tests, dosage optimization, drug screening and developmental areas [1, 5] and can help to speed the drug discovery process up which it takes nearly 10 years by shortening the animal experiments phase (Figure 1.1). Additionally, besides the shortening time, they require smaller amount of materials to fabricate and perform experiments and by means of those advantages, cost and required time are reduced.

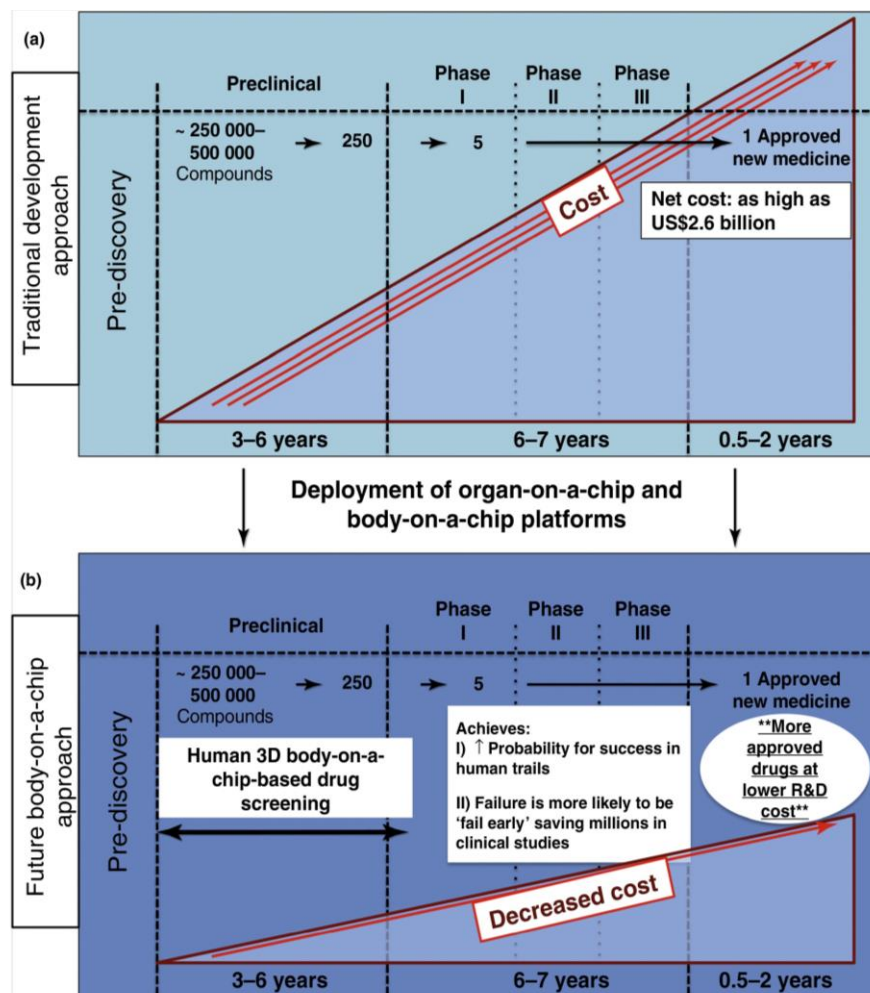


Figure 1.1: Potential improvements in the drug development pipeline as a result of the deployment of organ-on-a-chip and body-on-a-chip technologies into pharmaceutical research and development. (a) The current drug development pipeline requires many years and multiple billions of dollars to bring a drug to market. (b) Plugging in human-based biofabricated on-a-chip platforms into preclinical stages could drastically improve the efficiency of the drug development pipeline. (With permission from A. Skardal, T. Shupe, A. Atala, *Organoid-on-a-chip and body-on-a-chip systems for drug screening and disease modeling*, *Drug Discov. Today* 21(9) (2016) 1399–1411.)

1.2 Gradient Formation

Concentration gradients, has a key role in pharmaceutical applications as well as cell-based experiments because, cells can be manipulated by means of gradient [5, 7]. Microfluidics is one of the easiest ways to create a gradient since the controlling environmental factors is easier, and the potential for high-throughput experimentation [8]. In many researches, concentration gradient was created with different shapes of microchannels, such as S-shaped [7], Christmas-

tree shaped [9]. Concentration gradient also can be used in chemotaxis experiments [8]; For example, in the research that was done by Luster A. D. et.al, the white blood cells were investigated because of their abilities of detection and follow gradients [10].

1.3 Chemotaxis

Chemotaxis has been investigated for a long time [8] and is a natural movement changing behavior of organisms when there is a chemical gradient in their environment [11-14]. Chemotaxis behavior can be seen in different organisms such as cancer cells [12], microorganisms e.g. bacteria [14, 15] and *Caenorhabditis elegans* [16]. In human body, that behavior takes place in blood cells as Postlethwaite and Kang (1976) searched and in immune system cells' movement [13, 17]. Some traditional methods, such as transwell assay, Boyden chamber, under-agarose assay which are using free diffusion technique [18, 19], are used to observe chemotaxis behavior.

Sperm chemotaxis is the process where spermatozoa move towards an oocyte with help of its secretions [11, 20] (Figure 1.2). Different mechanisms which is thought that, are the combinations of chemotaxis, thermotaxis, and probably oviductal contractions [4, 21] and play a role in the guiding of sperm cells along the female genital tract and in mammals' system. Chemotaxis mechanism was firstly discovered in marine species [22] and during last decades, mechanism in mammals has gained much importance since Ralt et.al.(1994) mentioned the chemotaxis behavior in human follicular fluid, for the first time [23]. From the study that Sun et.al. (2003), it can be said that human and rabbit sperms have responded to a chemoattractant, and with the results they obtained, the question about whether chemotaxis is similar among other species was answered [24]. It has been thought that chemotaxis plays a key role during fertilization and it is important to observe sperm cells [25, 26]. Despite the fact that the content of the chemoattractants is uncertain, progesterone was proposed to be one of them.

Microfluidic devices can be used for chemotaxis experiments as well, because they provide stable chemoattractant gradient which has an important role in chemotaxis, and have a better ability to mimic the *in vivo* environment [8]. The studies which are done with microfluidic devices to observe the chemotaxis behavior is described more detailed in section 2.

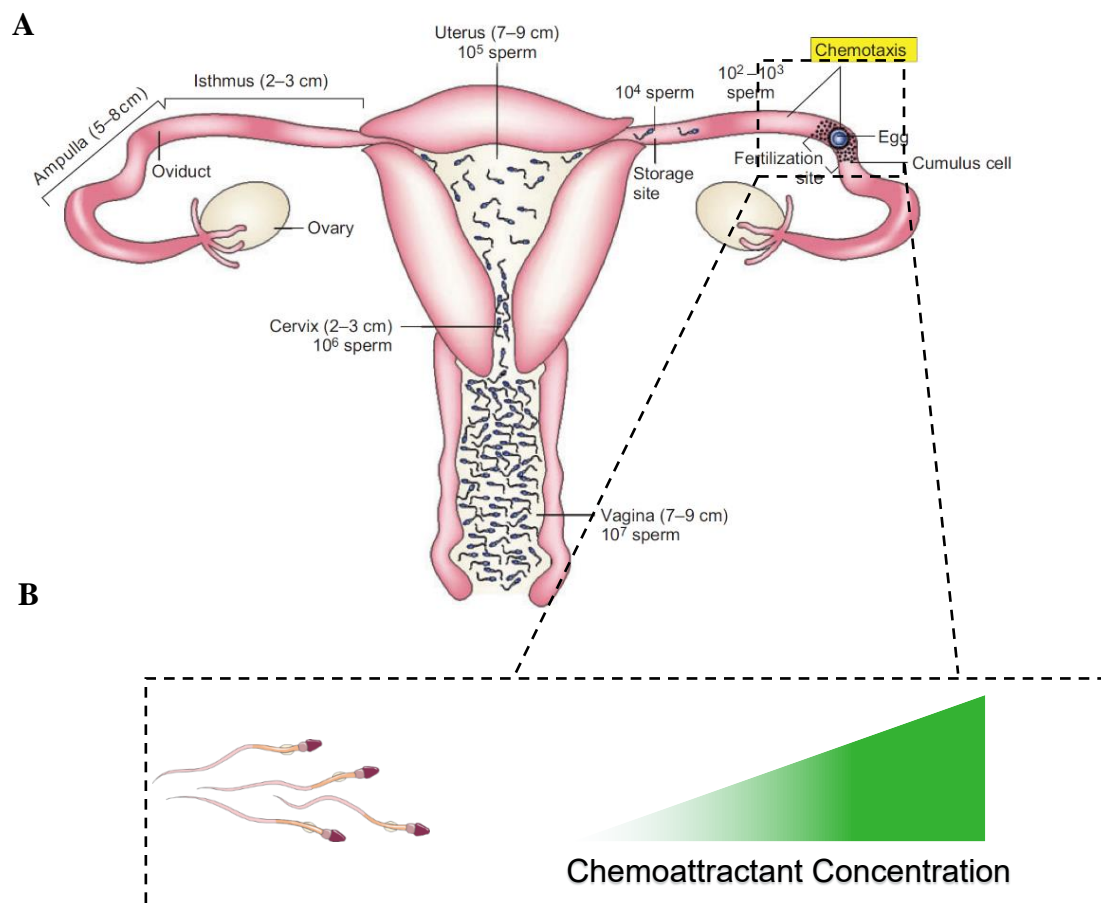


Figure 1.2: Chemotaxis movement in female genital tract (A) and schematic of this behavior towards gradient (B) (Figure was taken from U.B. Kaupp, N.D. Kashikar, I. Weyand, *Mechanisms of sperm chemotaxis*, *Annu Rev Physiol* 70 (2008) 93-117).

1.4 Hydrogels

Hydrogels are water-swollen and cross-linked materials which can be formed by covalent, ionic, van der Waals forces or mechanical bonds and can maintain their three-dimensional structure [27, 28]. They are widely used as biomaterials in biomedical engineering and bioengineering applications, due to their both physical and chemical properties such as swelling characteristics and diffusion behaviors. They can be used for mimicking extracellular matrix [29] as well as drug delivery materials [30]. Drug delivery has an importance in biomedical applications, because they improve most of the existing drugs [30].

1.4.1 Properties of Hydrogels

When the mechanical properties of hydrogels considered, swelling ratio is one of most important parameters that effects diffusion properties [30];

$$Q_M = \frac{M_s}{M_d} \quad (1.1)$$

where Q_M represents swelling ratio, M_s is weight of swollen hydrogel, while M_d shows the dry weight.

To understand the diffusion characteristics there are several theories such as hydrodynamic theory, obstruction theory, free volume theory [28, 31]. According to contents and scopes of those theories, free volume theory is the one suitable with this study since gelatin and agarose-based mixtures was used to perform diffusion studies. Free volume theory, briefly, takes the voids in a solution into consideration to calculate the solute diffusion [28, 31, 32]. In microfluidic devices especially for the flow-free devices, solute diffusion is a key parameter that has to be controlled over time [33]. The diffusion coefficient of the solute in liquid, D_0 , can be expressed as

$$D_0 \propto V\lambda \exp\left(-\frac{\gamma v^*}{v_f}\right) \quad (1.2)$$

where the V is the average thermal velocity, λ is the jump length equivalent to the solute diameter, v^* is the critical local hole free volume, γ is a numerical factor used for correction, and v_f is the average hole free volume per molecule in the liquid [28]. Also, this model can be written as

$$\frac{De}{D_0} = f(\overline{Mc}) \exp\left(-\frac{kR^2}{Q_M - 1}\right) \quad (1.3)$$

Peppas and Reinhart proposed [34]. In eqn (1.3), R is the solute hydrodynamic radius, k is a constant that is related to the structure of a polymer-solvent system, and $f(\overline{Mc})$ is a function of the molecular weight between cross-links [32].

1.4.2 Gelatin and Agarose

Gelatin is a natural protein-based biomaterial which is derived from collagen and one of the main component in extracellular matrix (ECM) [35, 36]. It is mostly preferable since it is biocompatible, biodegradable and water-soluble.

The source of gelatin can be porcine, bovine or fish tissues. It has high solubility in water, however it can be crosslinked with other hydrogels to enhance the mechanical properties, because of its similarity with ECM allows crosslinking [36]. *In vitro* applications in terms of cell culture environment, is one of the wide range applications of gelatin [37].

Agarose is also non-toxic natural polysaccharide that is derived from sea algae and is a water-soluble polymer [38, 39]. It was used for some microfluidic chip studies since it is a biocompatible polymer and it allows diffusion of molecules which can be nutrients for cell culture, yet in this work, it was used for progesterone diffusion [11, 40].

Since the combination of these two different hydrogels can improve mechanical properties, in some studies they were used in combination of different application areas such as microfluidics [41-43].

2. THEORETICAL BACKGROUND

This section describes the previous studies that are related with our research subject.

In the study that *Koyama et.al.* performed, chemotaxis assays of mouse sperm was observed with a PDMS-based microfluidic device which has 3 inlets and 3 outlets [3]. Chemoattractant gradient was formed with controlled flow and the velocity of the flow was optimized. Their design allows to collect positively responded sperms as well as negatively responded ones. When the chemotaxis experiments were performed, results showed that sperm cells have chemotaxis behavior.

According to study named ‘A microfluidic chemotaxis assay to study microbial behavior in diffusing nutrient patches’, device was designed and fabricated in order to perform chemotaxis assay to aquatic microorganisms [44]. They used PDMS and soft lithographic method. Three different marine bacterial isolates were used with various chemoattractants. Results showed that these marine species have chemotaxis behavior and their chemoattractant gradient is more precise when compared with literature. In addition, they claimed that this microfluidic device is compatible with other species rather than marine types.

Xie et.al (2010) fabricated a microfluidic device to observe sperm motility and chemotaxis behavior [4]. The microfluidic device was fabricated from PDMS with standard photolithography and micromolding procedure. Firstly, they optimized their design and width-length of the microchannel. Their device had one inlet, one straight channel and 2 outlets. They injected 25000 cells into the inlet pool and designed the experiments with adding cumulus cells which was used as chemoattractant source, into the other pools. According to classification in the article, this experimental setup can be defined as the ‘choice assay’ in which sperm cells choose where to go. As a result, they calculated a chemotaxis ratio and comparison between control group, results are significant and matched up with literature results.

In the study that *Ko et.al (2012)* performed, mouse semen samples were analyzed in terms of their chemotaxis behavior [20]. Sperm cells were separated with help of chemoattractant gradient in regard to their motility with a PDMS-based microfluidic device. Acetylcholine was used to attract mouse sperms. As a result, progressive sperm cells were separated easily with chemotaxis assay.

One of the researches that is related with chemotaxis was performed by *Chang et.al. (2013)* [11]. They used hydrogels which is a novel method to fabricate microfluidic device and compared sea urchins and mice's behaviors. They fabricated the device from agarose solution. Progesterone was used as a chemoattractant and gradient was formed. Even though their results showed that the progesterone may not has an effect on mice's sperm cells chemotactic movement, it was not stated certainly. But the microfluidic device was able to make a quantitative analysis of sperm movement in the chemoattractant gradient.

Zhang et.al. (2015) was also investigated spermatozoa chemotaxis with generating a gradient in their microfluidic device [45]. They fabricated easy-handle diffusion chip which has six channels surrounding a hexagonal pool where progesterone gradient was formed. 2 Different concentrations of progesterone were used, and they observed obvious chemotaxis behavior for both concentrations, similar to previous studies.

Hussain et.al. (2016) was used microfluidic device which was fabricated from PDMS to observe effect of sperm chemotaxis on male fertilization in sea urchins [46]. To make a comparison, firstly they removed chemoattractant from eggs and then measured difference in fertilization. The microfluidic device was designed and used for creating controlled chemoattractant gradient. Relation between sperm movement towards chemoattraction and male fertility was correlated in this study. Also, they observed the chemotaxis behavior of sperm cells towards a chemoattractant gradient.

In light of the previous studies' findings and inadequacies, in this study, we developed a novel flow-free hydrogel-based microfluidic device to assess the sperm chemotaxis with formation of a chemoattractant gradient. Our microfluidic device was fabricated from gelatin/agarose hydrogel mixture solution. Some parameters, for example gradient formation time and hydrogel solution composition, were optimized, followed by the chemotaxis experiments which were performed with boar's spermatozoa and obtained good chemotactic response.

3. METHODOLOGY

This chapter focuses on the main instruments used in this work. An outline of the working principles of the laboratory equipment will be given first to understand the main restrictions of experiments.

3.1 Instrumentation

In this section, the instruments that were used during experiments will be described.

3.1.1 Oxygen Plasma Cleaner

In microfluidic applications surface modification can be applied for different types of surfaces such as PDMS, glass etc. For that purpose, generally chemical or plasma oxidation methods are used. In this work, the combination of chemical surface modification and plasma cleaning were used.

Plasma cleaning is a process that removes impurities and/or contaminants from the surfaces. It uses the fourth form of matter which is plasma. Plasma is obtained from energetic gaseous phase by means of radiation [47]. In that environment, ions, electrons and free radicals can be found.

In this research, the plasma cleaner from Femto Science Inc., CUTE model was used. It's a low-pressure plasma cleaner and can be used for either cleaning or modification like increasing the hydrophilicity of a surface.

3.1.2 Microscopes

In this work, two different types of microscopy techniques were used; fluorescence and light microscopy.

Fluorescence microscopy is one of the most preferred techniques in biomedical applications. There are several types of methods that use fluorescence materials, for example attaching a fluorochrome to an antibody and fluorescein isothiocyanate (FTIC) immunofluorescence technique [48]. However, basically, every method consists of a material which can absorb and reflect light (fluorescence) and a microscope to observe it.

EVOS FL (Invitrogen, a ThermoFisher Scientific company) was used as a fluorescence microscope. It's a digital inverted microscope and can be used not only for fluorescence applications, but also cell culture imaging. For fluorescence imaging, EVOS uses both mechanical and software controls.

Even though there are several types of light microscopes, in this research inverted microscope was used. It's a type that light source is at the top and the objectives are below the plate that sample stays on. Inverted microscopes are suitable for cell culture applications. Nikon Eclipse TE2000-U (Figure 3.1) was used as an inverted microscope with combination of Photron Fastcam SA3 high speed video system (10x phase contrast objective at exposure of 1ms).

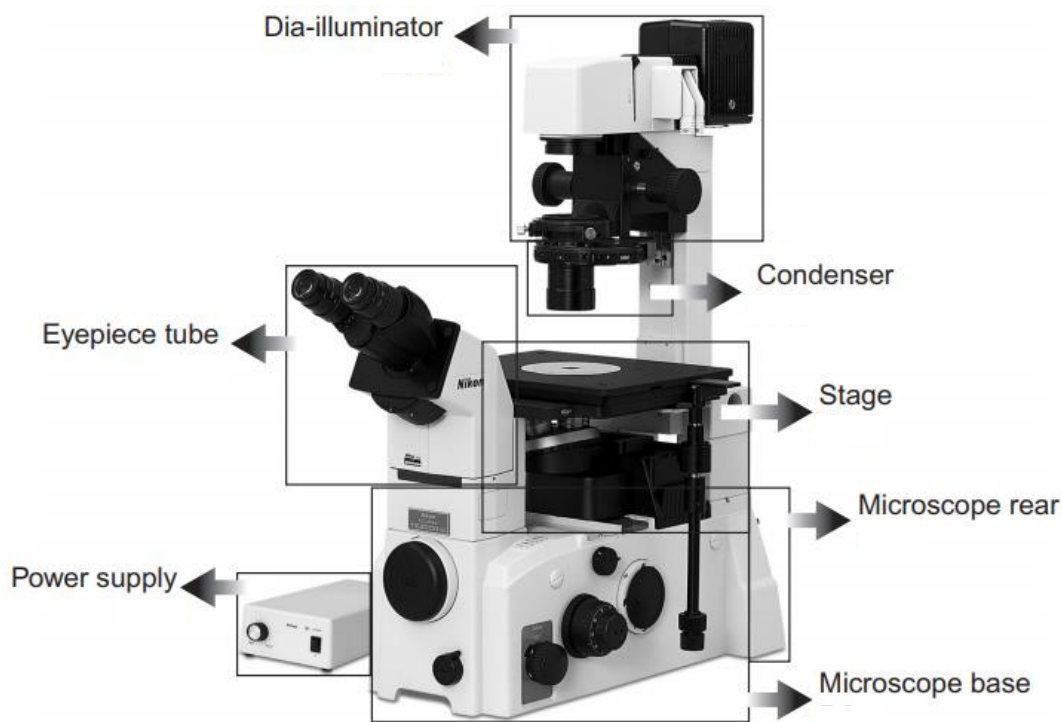


Figure 3.1: Schematic of general structures of Nikon TE2000-U microscope [49]

3.1.4 Punches

Harris Uni-Core 3 mm punches was used to create holes in the hydrogel-based microfluidic chips. These are inexpensive materials and can be used different purposes. Generally thin and soft samples for instance gels, dried blood cards are suitable for those punches.

3.2 Method

In this section, the experiments which were done to observe spermatozoa behavior, are described.

3.2.1 PDMS Mold Fabrication

To fabricate hydrogel-based microfluidic device the design from the previous studies was used (Figure 3.3). Our design has 3 channels (one middle channel and 2 side-channels) and 6 inlets/outlets. Diameter of the inlet/outlets which belong to the middle channel is 4 mm and others are 2 mm and the depth of the channels is 350 μm . Mastermolds (30 mm x 20 mm x 4 mm, positive mold) were 3D printed with that design on the top surface.

Then, PDMS molds were fabricated from 3D printed ones with PDMS solution and curing agent (1:10 ratio, respectively). Approximately 5 or 6 grams of PDMS was put into the 15 ml volume-tubes and curing agent was added. This was then mixed until a homogenous solution was obtained. To eliminate the air bubbles which mixing caused, tube was placed into the desiccator for 20 minutes.

3D printed molds were become containers for PDMS solution with using tape. After degassing period, the PDMS solution (negative mold) was poured onto the 3D printed molds (positive mold). Molds were put in the oven at 60 $^{\circ}\text{C}$ and left to cure for 2 or 3 hours. After curing, solid PDMS molds were peeled off from the 3D printed molds and used in further experiments.

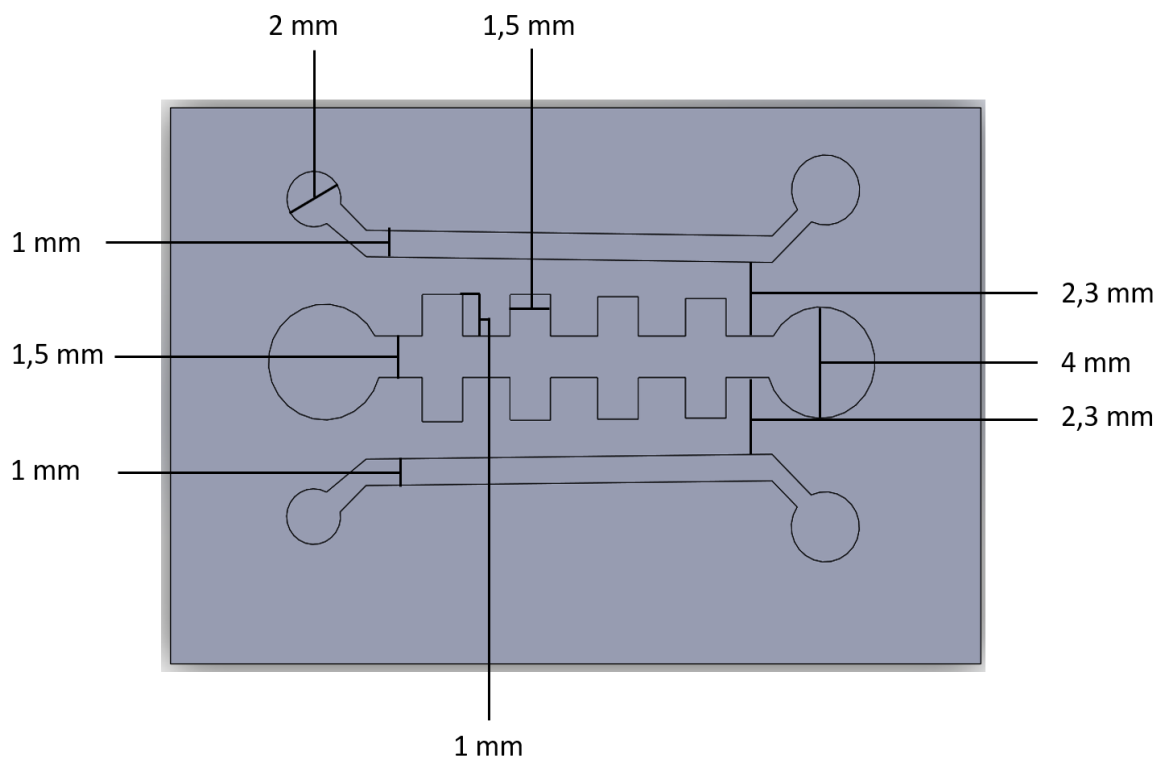


Figure 3.3: Design of the microfluidic device. Microfluidic chip has 3 channels (one middle channel and 2 side-channels) and 6 inlets/outlets. Diameter of the inlet/outlets which belong to the middle channel is 4 mm and others are 2 mm and the depth of the channels is 350 μm .

3.2.2 Hydrogel Solution Preparation

Microfluidic chips were fabricated from combination of 2 hydrogel solutions. For that purpose, hydrogel solution was prepared with dissolved agarose and gelatin. The reason to use hydrogels to create a gradient is, due to their diffusion properties.

Agarose (Agarose for routine use, A9539, Sigma Aldrich) was dissolved in PBS at 85 $^{\circ}\text{C}$ under stirring to prepare 1% (w/v) solution. Gelatin solution (8% w/v) (Gelatin from porcine skin, G1890 Sigma Aldrich) was also prepared same as agarose mixture. To prepare the gelatin/agarose mixture (8:1 (w:w)), firstly, gelatin (16% w/v) and agarose (2% w/v) were dissolved in PBS separately and mixed with 1:1 (v:v) ratio under stirring and heating (at 85 $^{\circ}\text{C}$) for approximately 20 minutes [39].

3.2.3 Hydrogel Chip Fabrication and Bonding

The prepared solutions (see section 3.2.2) were poured into the PDMS molds (see section 3.2.1) and left to cure until become solid in the refrigerator ($\sim+4^{\circ}\text{C}$). Afterwards, inlets and outlets were punched out from hydrogel with a 3 mm punch (Harris Uni-Core, 3mm punch) (Figure 3.4).

For the bonding process, glass slides were chemically functionalized on their surfaces (Figure 3.5). Firstly, glass slides were cleaned with a plasma cleaner (Femto Science, Plasma System CUTE). Then, (3-Aminopropyl)triethoxysilane (APTES) solution (3% v/v) was prepared with miliQ water. Cleaned glass slides were dipped into the APTES solution and left for 30 minutes which this step allows amino groups to bound on the glass surface covalently. Afterwards, glass slides were dipped into glutaraldehyde solution (10% v/v) which was prepared with PBS. Glutaraldehyde treatment allows aldehyde groups to bind to the amino groups that were bonded to the surface with APTES solution treatment. Glass slides were washed with deionized (DI) water after every step. At the end of the surface coating, DI water was removed from glass surface with strong air flow and hydrogel chips were bonded with glass slide.



Figure 3.4: General steps of hydrogel solution preparation. Firstly, the hydrogel solution mixture was prepared and poured into PDMS molds. After solidifying step, inlets/outlets were punched out from the hydrogels.

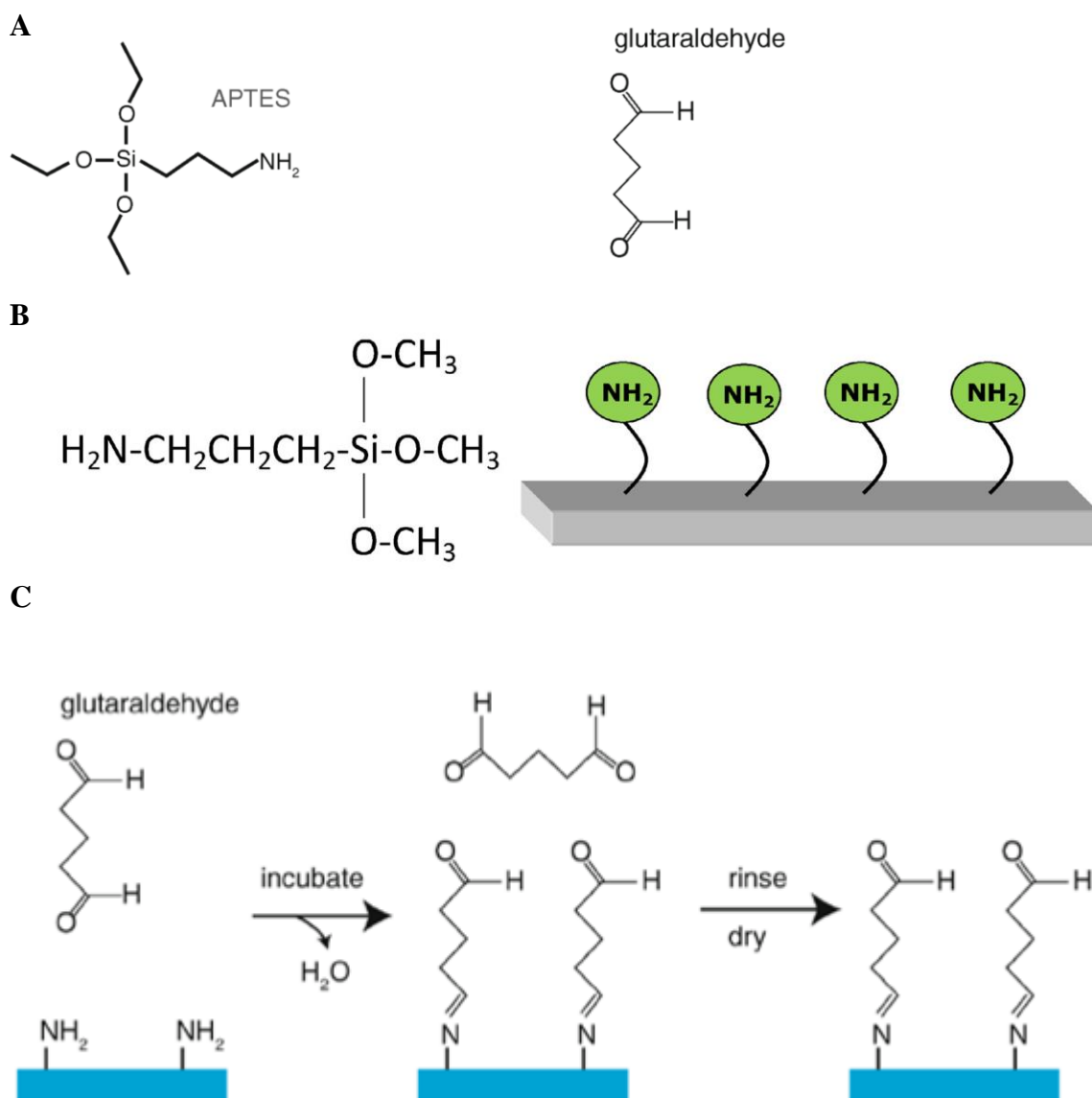


Figure 3.5: Chemical structure of (3-Aminopropyl)triethoxysilane (APTES) and glutaraldehyde (A). First step of the APTES coating on the glass surface which is treating the surface with APTES and creating open NH_2 groups (B). Glutaraldehyde application on the NH_2 coated surface (C) (Figure was modified from *M.E. Marques, A.A.P. Mansur, H.S. Mansur, Chemical functionalization of surfaces for building three-dimensional engineered biosensors, Applied Surface Science 275 (2013) 347-360* and *M.P. Nicholas, L. Rao, A. Gennerich, Covalent immobilization of microtubules on glass surfaces for molecular motor force measurements and other single-molecule assays, Methods Mol Biol 1136 (2014) 137-69*).

3.2.4 Cell Viability Experiments

Cell viability or cytotoxicity assays are generally used to measure the toxicity level of chemicals. In this research, those assays were used to calculate the viability rate and duration of spermatozoa in the fabricated chips (see section 3.2.3)

Sperm cells were stained with Live/Dead Sperm Viability Kit® (Molecular Probes, (L-7011)) to calculate the viability percentages. This assay was designed especially for sperm cells and contains a membrane-permeant nucleic acid stain (SYBR®14 dye) and propidium iodide (PI) for the conventional dead-cell stain. Since the both dyes label DNA, different cell parts can be dyed and look fluorescent. At the end of the staining procedure, alive sperm cells will look green because of the normal membrane structure, while the dead cells since they have damaged cell membrane will look red.

Figure 3.6 shows the general steps of the cell viability assay. According to their procedure, SYBR®14 solution was diluted 50 times with DI water and mixed with 1 mL sperm cells solution. After 10 minutes incubation time, propidium iodide (5 µL) was added and incubated 10 minutes again and observed with fluorescence microscopy (EVOS FL, Invitrogen). Results were analyzed with ImageJ (version 1.52a) while setting the threshold to a suitable ratio to distinguish the live/dead cells by using ‘analyze particle’ function. Afterwards, viability proportions were calculated among all counted cells.

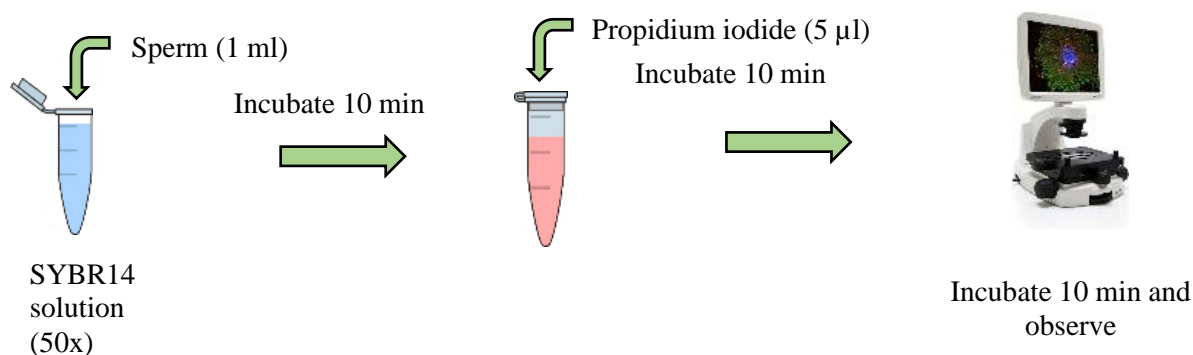


Figure 3.6: The schematic of the cell viability assay general steps. Firstly, sperm solution was mixed with 50x SYBR14 dye and incubated for 10 minutes to have a proper binding. 10 minutes after the solution was mixed with 5 µl propidium iodide, the microfluidic chip was observed with a fluorescence microscopy and the images were analyzed with ImageJ.

3.2.5 Gradient Trials

Gradient formation experiments were performed in order to achieve a constant and uniform gradient around the middle channel since the main purpose of this research is to observe spermatozoa behavior under a chemoattractant gradient.

Firstly, hydrogel-based chips were fabricated (section 3.2.3) and then gradient experiments were performed in these microfluidic chips. To optimize the duration of gradient formation, experiments were performed with fluorescein sodium salt solution (0,005%, Diffusion coefficient: $4,25 \times 10^{-6} \text{ cm}^2 \text{ s}^{-1}$, MW: 376,27 g/mol [51]) which has a nearly same molecular weight as progesterone (MW: 314,46 g/mol). Fluorescein sodium salt solution were added one of the side-channels (Figure 3.7) and the channels were observed with fluorescence microscopy with a 10x objective until the gradient reaches middle of the middle channel. Results were analyzed with ImageJ with 'Plot Profile' function and graphs were drawn with R (Version 1.1.463), Knime analytics platform (version 3.6.2) and Microsoft Excel.

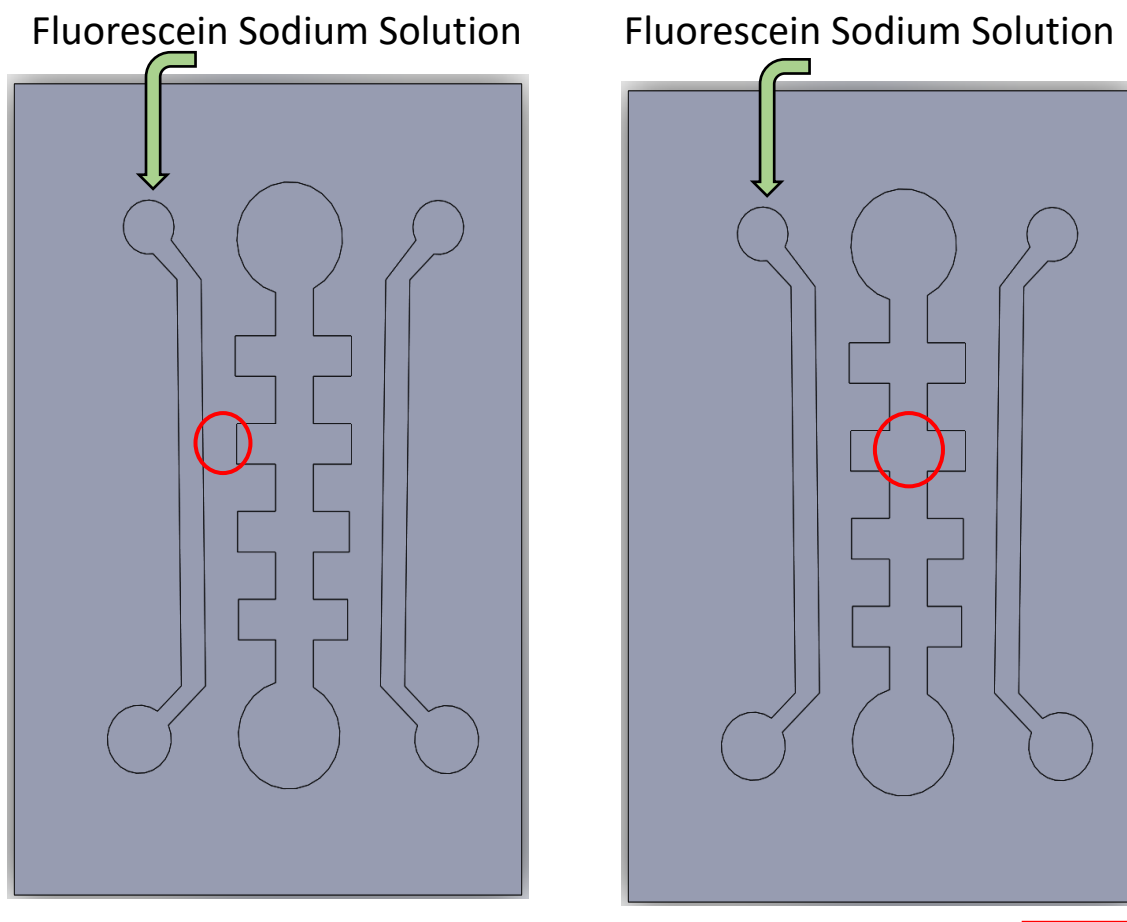


Figure 3.7: Fluorescein solution was injected to one of the side channels and the area between side channel and middle channel, and the middle side of two side-chambers were observed with fluorescence microscopy. Red circles show the observed areas of the fabricated hydrogel-based microfluidic devices. Scale bar is 4,75 mm.

3.2.6 Progesterone Experiments

According to the theory, spermatozoa move towards a chemoattractant which is generally a hormone. To prove that theory, chemotaxis experiments were done with progesterone hormone.

1 μM progesterone solution was prepared from a stock solution which has 8 $\mu\text{g/ml}$ concentration. Progesterone solution was injected into one of the side-channels and waited approximately 160 minutes which was optimized before (see section 3.2.5). Afterwards, the chips were put onto the heating plate (37 $^{\circ}\text{C}$) until the channels were heated up (approximately 5 minutes). 10 μL from the sperm cells solution (2×10^6 cell/ml) were injected into the middle

channel and observed with light microscopy (Nikon Eclipse TE2000-U). Videos (3 seconds for each side-chamber) were taken with Photon Fastcam SA3 using a 10x phase contrast objective at auto-exposure for the 6 different side-chambers. Results were analyzed for spermatozoa's movement behaviors and the number of the spermatozoa in the side-chambers with ImageJ's MTrackJ and Cell Counter plugins, respectively.

Moreover, to express the results simply, a ratio was defined which is called '**chemotaxis index**'. It is the proportion of the number of cells in progesterone-applied side of the middle channel vs. the other side of middle channel (Figure 3.8). To perform chemotaxis experiments, three different setups (two different progesterone application channel and 1 control group which has no progesterone effect) were prepared (Figure 3.9).

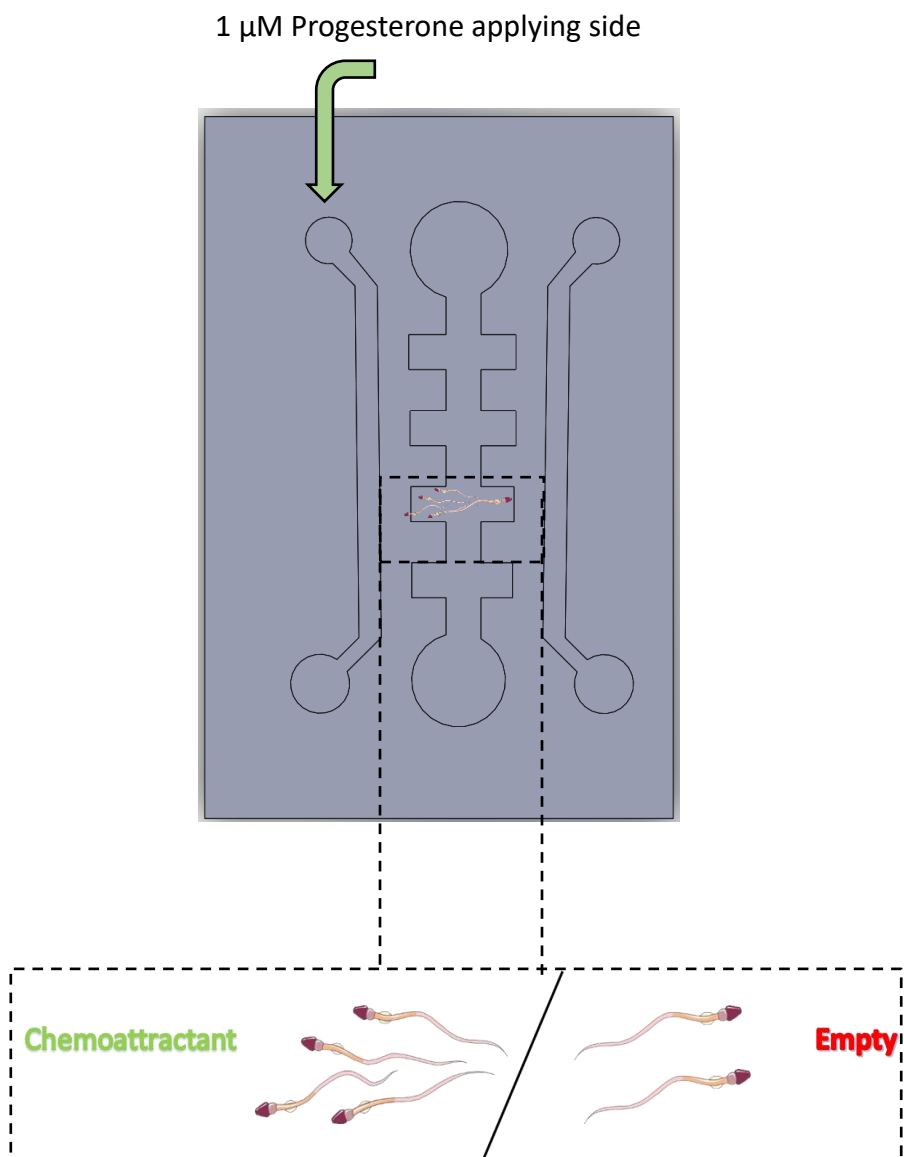


Figure 3.8: Sketch of calculation of the chemotaxis ratio. 1 μ M progesterone solution was injected into one of the side channels and then waited until create a gradient. Afterwards, spermatozoa solution (2×10^6 cell/ml) was injected into the middle channel from one of the inlets. The ratio was calculated according to the sperm cells number in every side chamber.

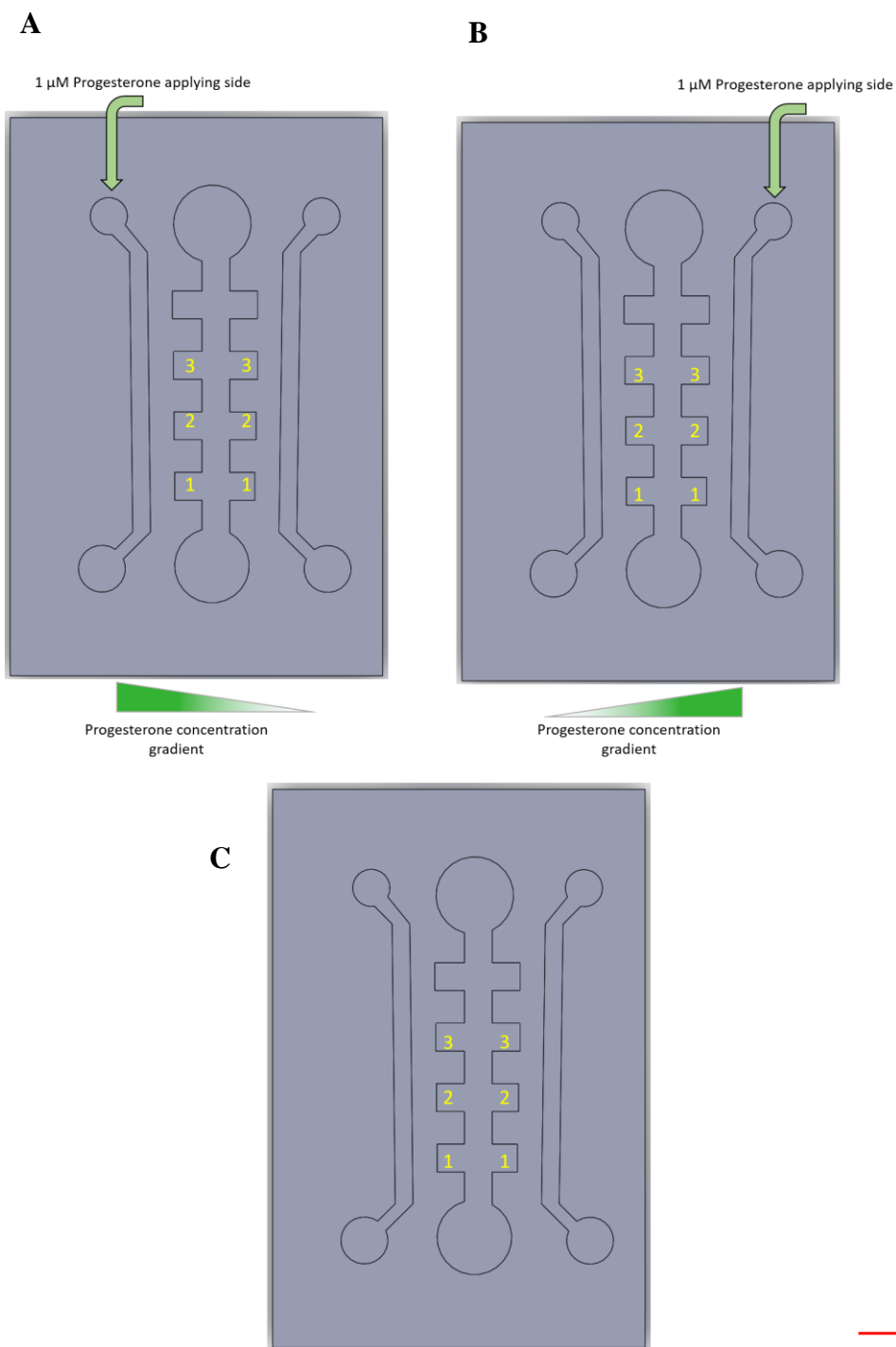


Figure 3.9: 3 different experiment groups to observe spermatozoa's chemotaxis behavior. Firstly, progesterone was applied from the left side-channel (A) and afterwards application side changed to right side-channel (B). For the control group, chips were not treated with progesterone (C). Scale bar is 4,75 mm.

3.2.7 Statistical Analysis

In chemotaxis experiments, chemotaxis index values for 6 different observed side-chambers were calculated (section 3.2.6) and compared using t-Test: Two-Sample Assuming Unequal Variances was done with Microsoft Excel data analysis function. $p < 0,05$ was considered as a statistically significant difference.

4. RESULTS AND DISCUSSION

4.1 Optimization of Hydrogel Preparation

The microfluidic device was fabricated as hydrogel-based. The hydrogel solution prepared as described in section 3.2.2. In previous studies, agarose was used [11], however, it has been seen that viability of sperm cells did not remain long enough to perform further experiments. Therefore, gelatin was used as another option to fabricate microfluidic device. The concentration of gelation solution was optimized while trying different concentrations varying between 7% (w/v) and 10% (w/v). For high concentrations of gelatin, it gets too solid and sticky and this makes chips nonworkable. On the other hand, low concentrations of gelatin like 7% (w/v), it does not become solid to be able to work with. As a result, 8% (w/v) was chosen and chips were fabricated following the protocol in section 3.2.3.

For the progesterone experiments, however, chips are needed to heat up to 37 °C to mimic the human body temperature. Since the melting point of the gelatin solution was below body temperature (35 °C [41]) chips melted. To overcome that complication and keep the viability ratio as required, gelatin/agarose mixture (8:1 w:w) was used to fabricate microfluidic devices. The mixture was prepared dissolving agarose and gelatin separately and then mixing both of them under stirring and heating. The only problem with that method is, if the mixing is not adequate, the structure of the chips may not be uniform and/or homogenous and they will melt during progesterone experiments, yet it is a quick and efficient method.

4.2 Viability

Viability test was performed according to Live/Dead Sperm Cells Viability Kit's manual. At the end of the procedure, live cells are stained green as well as dead cells are stained red. The percentages between live and dead cells was calculated for 20 minutes observation time with help of ImageJ's particle analyzing function (Figure 4.1-B).

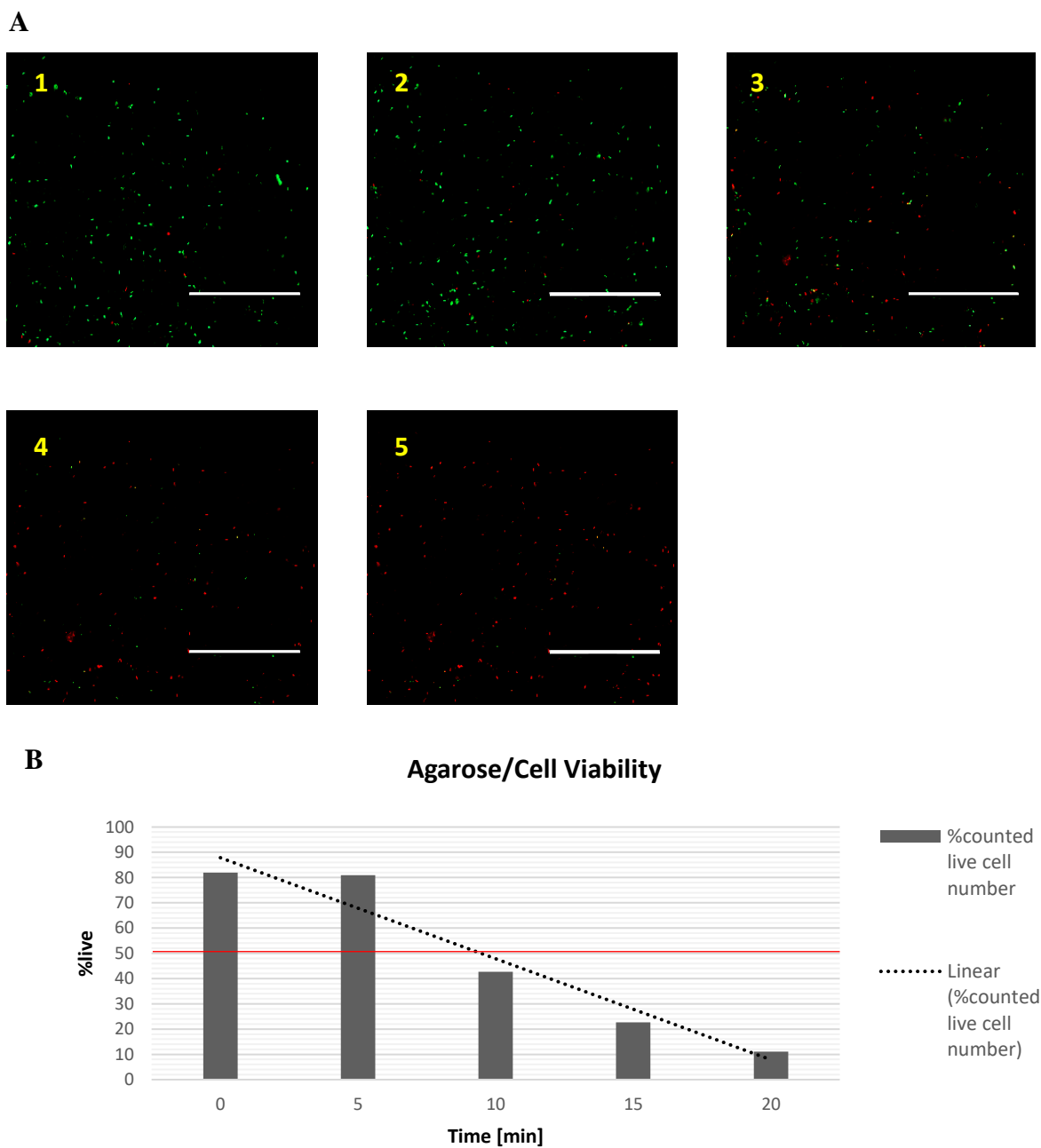
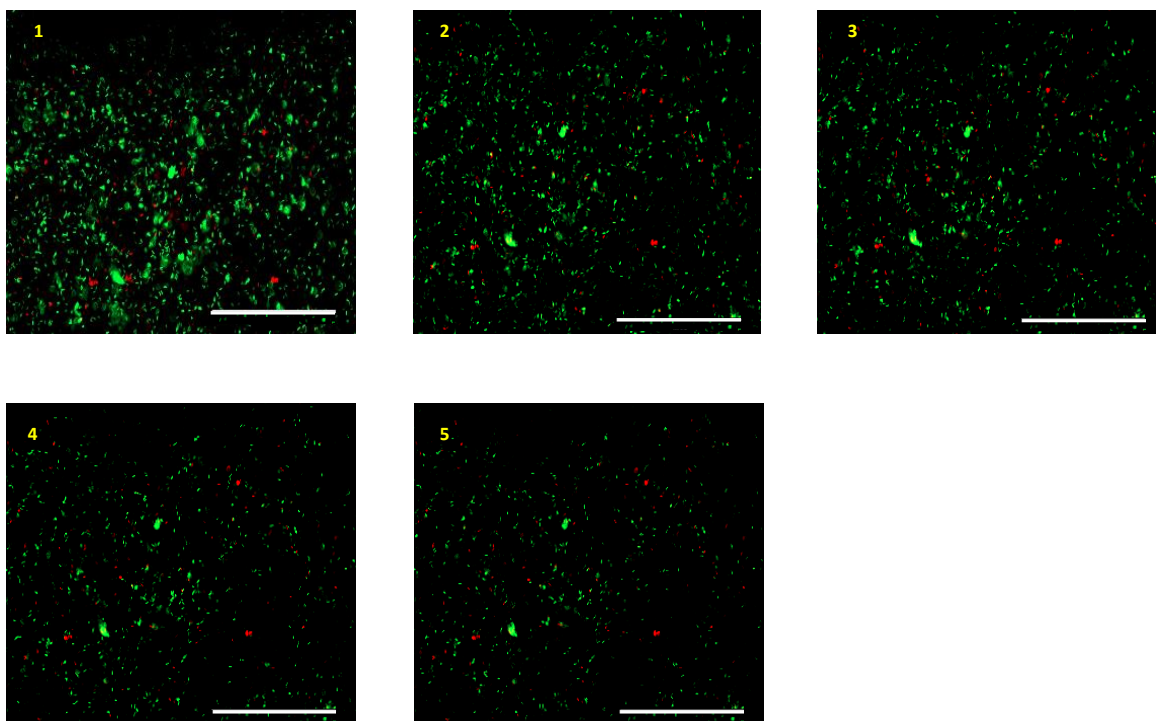


Figure 4.1: Viability results of hydrogel-based microfluidic device which was made from agarose. Fluorescence images of the live and dead spermatozoa within 20 minutes observation time (A). Sperm cell at the beginning (1), at 5 minutes (2), 10 minutes (3), 15 minutes (4) and 20minutes (5). Cell viability percentages graph of the alive and dead sperm cells (B) and red line shows the 50% of ratio. Scale bar is 400 μ m.

When the chips were fabricated from agarose, results showed that number of dead sperm cells become higher than the live cells after 5 minutes and at the end of the 20 minutes, almost there is no live cells (Figure 4.1). Also, after 10 minutes, the live/dead cell ratio was under 50% which is not sufficient time to obtain accurate results from chemotaxis experiments. On the other hand, gelatin-based chips have the highest living cell ratio (Figure 4.2). Throughout 20 minutes, all the ratios are above 50% which makes the gelatin best option in terms of viability for chemotaxis tests. However, because of the low melting point problem, solely gelatin was not preferred for the further experiments.

With taking into consideration of advantages and disadvantages of gelatin and agarose, the mixture of these hydrogels was used. The live/dead cell ratios were lower than the gelatin's, but still they were higher than 50% for a certain duration as required (Figure 4.3).

A



B

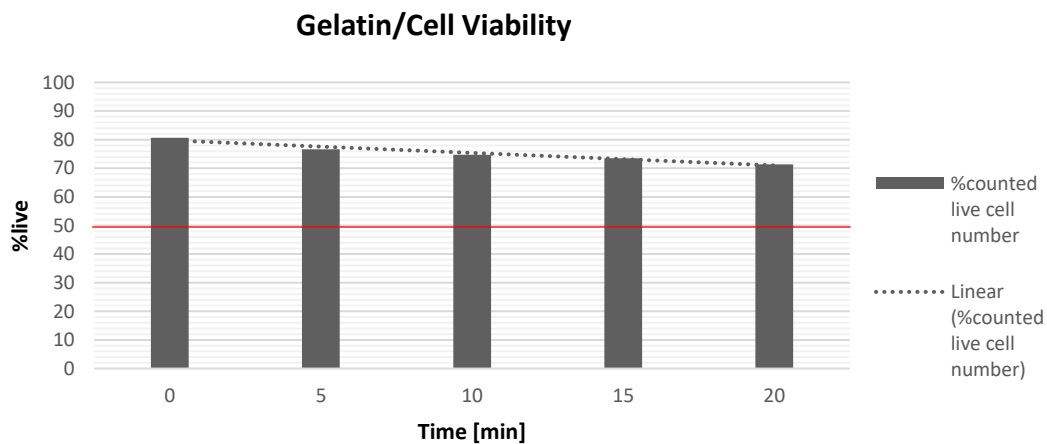


Figure 4.2: Viability results of hydrogel-based microfluidic device which was made from gelatin. Fluorescence images of the live and dead spermatozoa within 20 minutes observation time (A). Sperm cells at the beginning (1), at 5 minutes (2), 10 minutes (3), 15 minutes (4) and 20minutes (5). Cell viability percentages graph of the alive and dead sperm cells (B) and red line shows the 50% of ratio. Scale bar is 400 μ m.

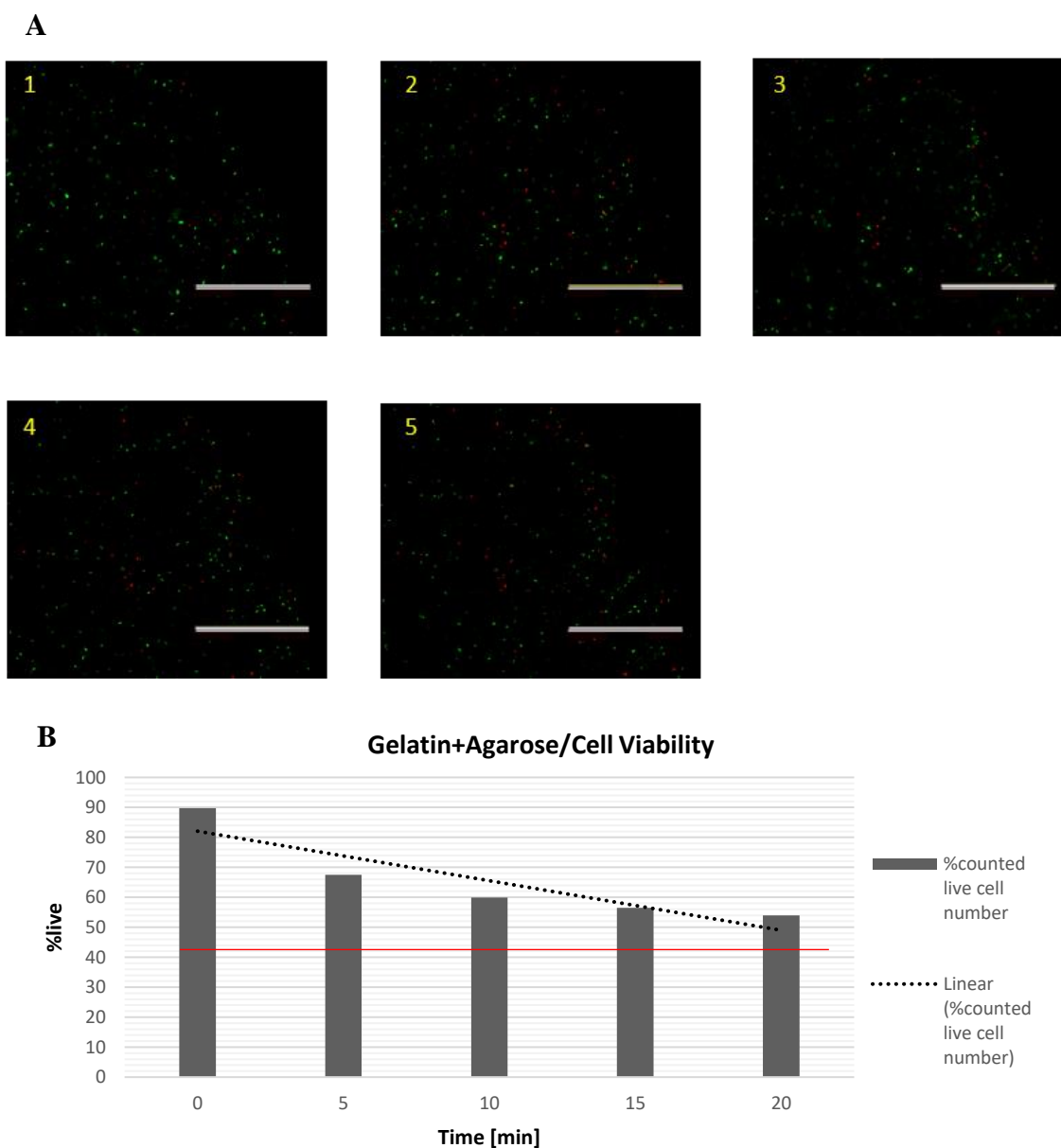


Figure 4.3: Viability results of hydrogel-based microfluidic device which was made from gelatin/agarose mixture. Fluorescence images of the live and dead spermatozoa within 20 minutes observation time (A). Sperm cell at the beginning (1), at 5 minutes (2), 10 minutes (3), 15 minutes (4) and 20minutes (5). Cell viability percentages graph of the alive and dead sperm cells (B) and red line shows the 50% of ratio. Scale bar is 400 μm .

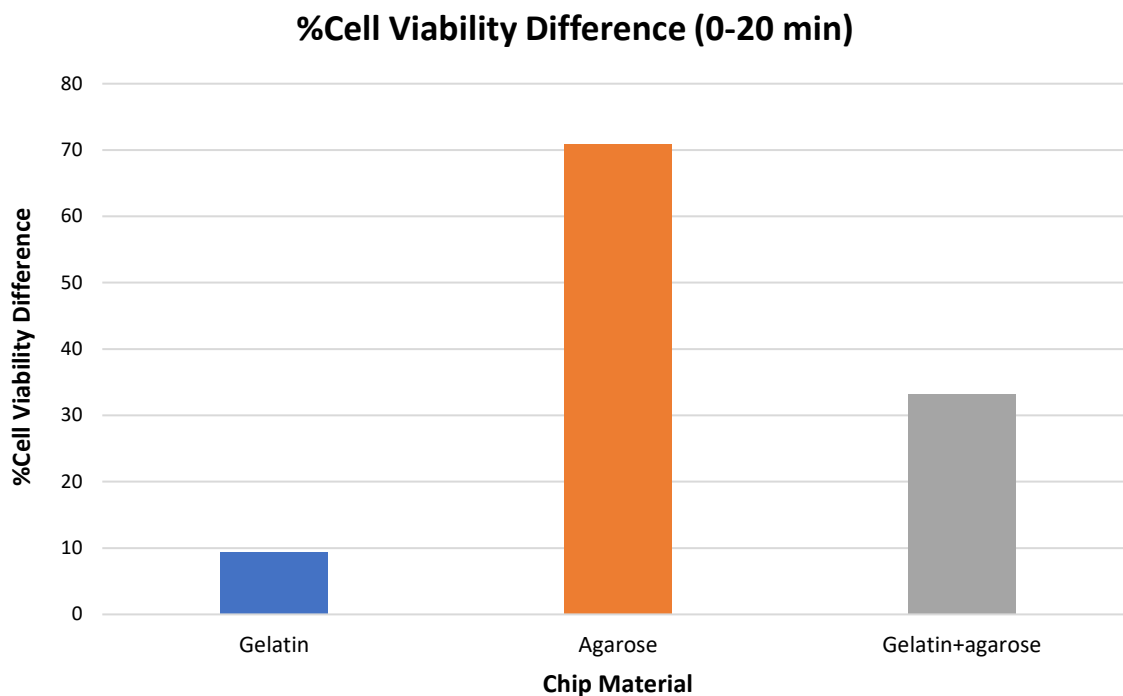


Figure 4.4: Comparison of three different hydrogel solutions' viability rate within 20 minutes.

Figure 4.4 shows the percentage differences from 0 minute until 20 minutes. Data was generated from the live/dead percentage values from Figure 4.1, Figure 4.2 and Figure 4.3. Since the bars represent the difference from at the beginning until at the end of the experiments, the bigger difference means that cells died faster when compared to other hydrogel types. Therefore, it can be said that spermatozoa die faster in agarose-based chip and fluorescence images also support that statement. On the other hand, for the gelatin/agarose mixture, sperm cells can stay alive mostly (less than 40% death rate) for at least 20 minutes.

In conclusion, not only for the percentages, but also melting temperatures, the mixture is a good material to fabricate chips and it was used for the future experiments.

4.3 Optimization of Gradient Formation Time

Gradient experiments were performed with hydrogel chips which were prepared as described in section 3.2.3. The purpose for that experiment is that creating progesterone gradient in the middle of the middle-channel. Therefore, fluorescein sodium salt solution (0,005%, MW: 332g/mol) was preferred since its' molecular weight is comparable with progesterone's (MW: 314g/mol).

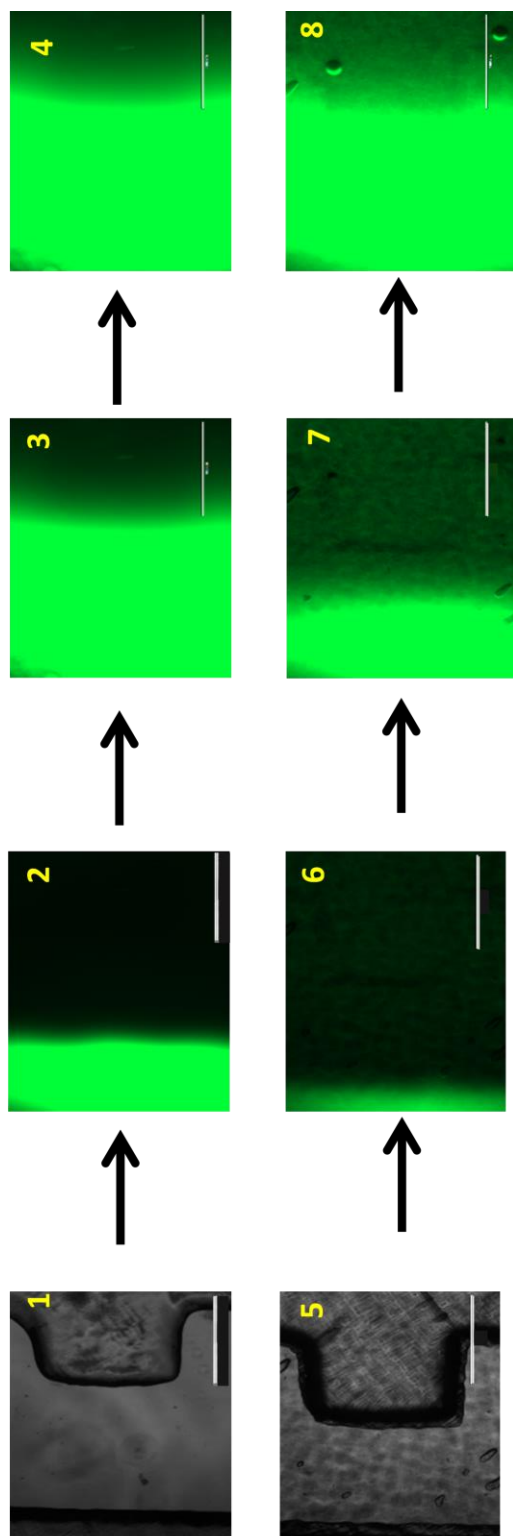


Figure 4.5: Agarose and gelatin/agarose gradient formation time experiment with sodium salt fluorescein solution. (1) side chamber before the experiment for agarose-based chip, (2) 5 minutes after applying fluorescein solution for agarose-based chip, (3) 10 minutes after applying fluorescein solution for agarose-based chip, (4) 15 minutes after applying fluorescein solution for agarose-based chip. (5) side chamber before the experiment for gelatin/agarose-based chip, (6) 5 minutes after applying fluorescein solution for gelatin/agarose-based chip, (7) 10 minutes after applying fluorescein solution for gelatin/agarose-based chip, (8) 50 minutes after applying fluorescein solution for gelatin/agarose-based chip. Scale Bar: 1000 μm .

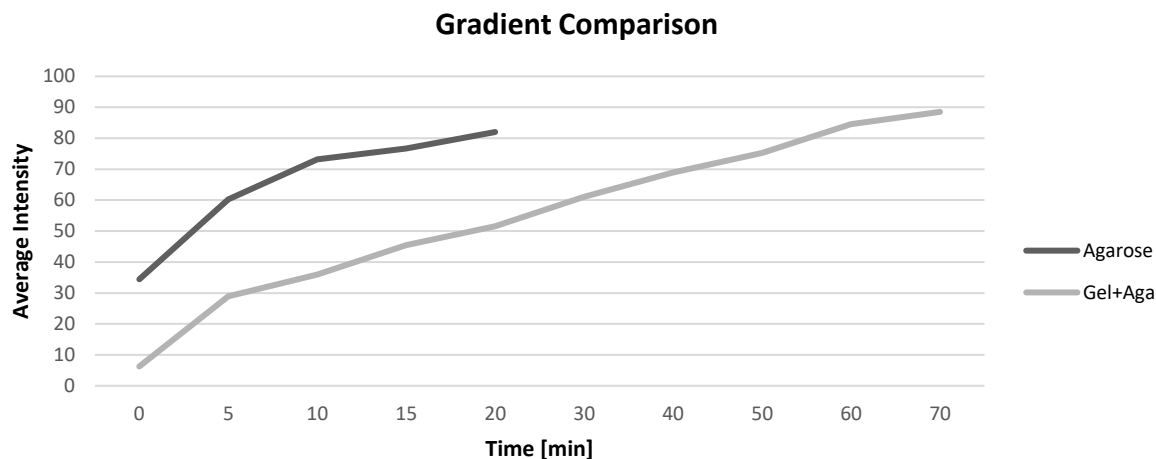


Figure 4.6: Comparison of average intensity for the agarose and gelatin/agarose chips for the area that between middle channel and side channel (See Figure 3.7).

It can be seen that, for the agarose-based microfluidic device (Figure 4.5), the diffusion rate is faster than the gelatin/agarose mixture. They reach the same intensity (Figure 4.6) at different times for example, for intensity value 60, agarose reaches that point at within 5 minutes, while gelatin/agarose mixture-based chips reach that intensity at 30 minutes. For agarose it is 15 minutes, while it is 50 minutes for gelatin/agarose mixture. Additionally, the slopes from the Figure 4.6 show the diffusion rate and it is clear to say that agarose has faster diffusion rate.

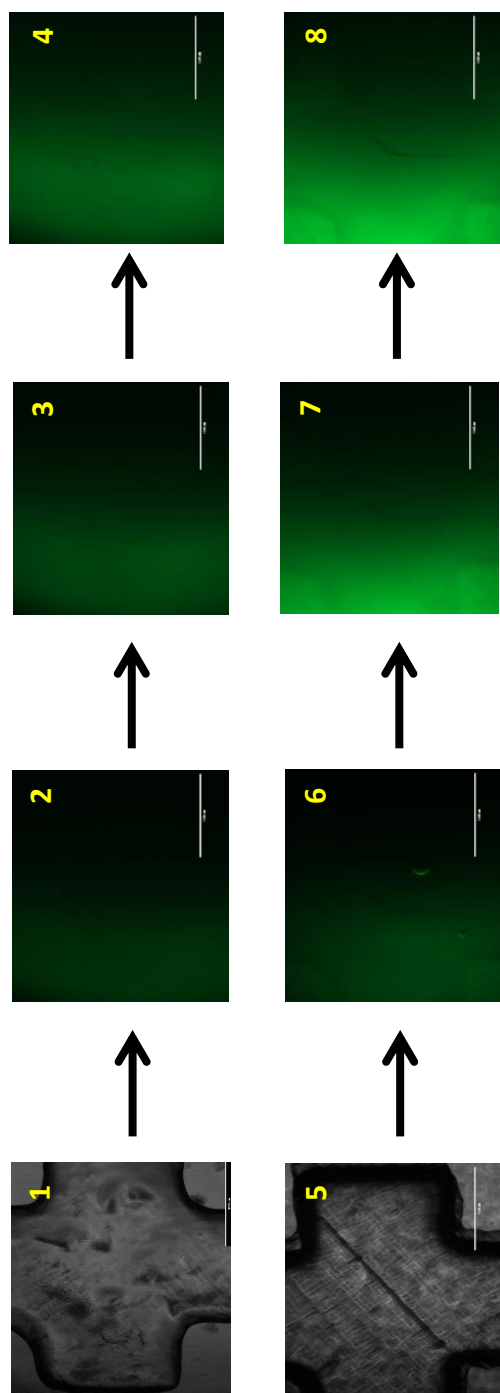


Figure 4.7: Agarose and gelatin/agarose gradient formation time experiment with sodium salt fluorescein solution. (1) middle channel before the experiment for agarose-based chip, (2) 5 minutes after applying fluorescein solution for agarose-based chip, (3) 10 minutes after applying fluorescein solution for agarose-based chip, (4) 15 minutes after applying fluorescein solution for agarose-based chip. (5) middle channel before the experiment for gelatin/agarose-based chip, (6) 5 minutes after applying fluorescein solution for gelatin/agarose-based chip, (7) 10 minutes after applying fluorescein solution for gelatin/agarose-based chip, (8) 50 minutes after applying fluorescein solution for gelatin/agarose-based chip. Scale Bar: 1000 μm .

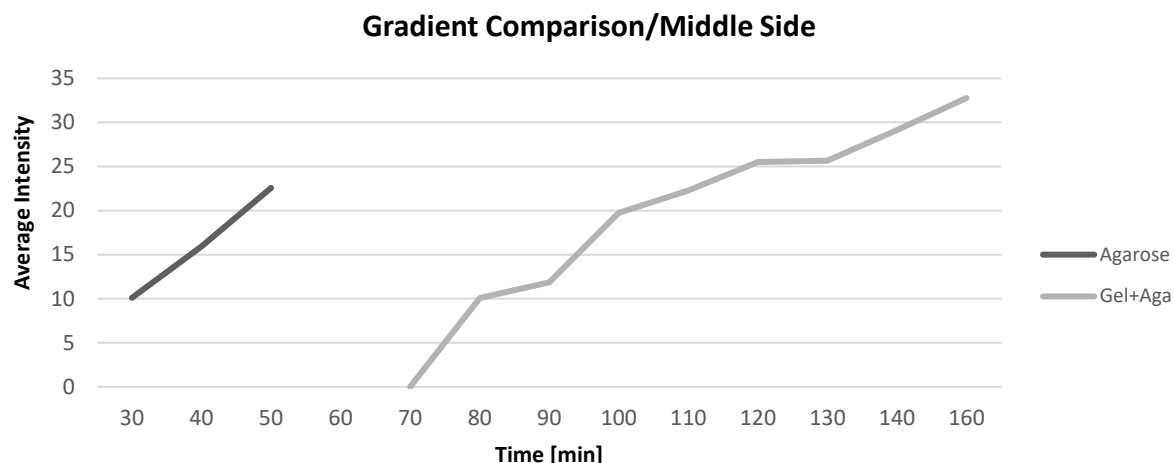


Figure 4.8: Comparison of average intensity for agarose-based and gelatin/agarose-based chips for the middle channel.

When the observed area was changed, the average intensity values decreased since the source is away (Figure 4.7, Figure 4.8). The required time to achieve the same intensity value for those 2 different chip materials, is very different (Figure 4.8). To form a proper gradient, 160 minutes is required for gelatin/agarose, whilst approximately 50 minutes is enough for agarose chip. Consequently, even though the diffusion process is faster for agarose chips, when the viability results are considered (Figure 4.4), gelatin/agarose mixture-based chips are used for progesterone experiments.

4.4 Progesterone Experiments

To observe the chemotactic behavior of spermatozoa, chemotaxis experiments were performed with progesterone hormone gradient. For that reason, a ratio was defined which is called '**chemotaxis index**'. It is the proportion of the number of cells in progesterone applied side of the middle channel vs. the other side of middle channel.

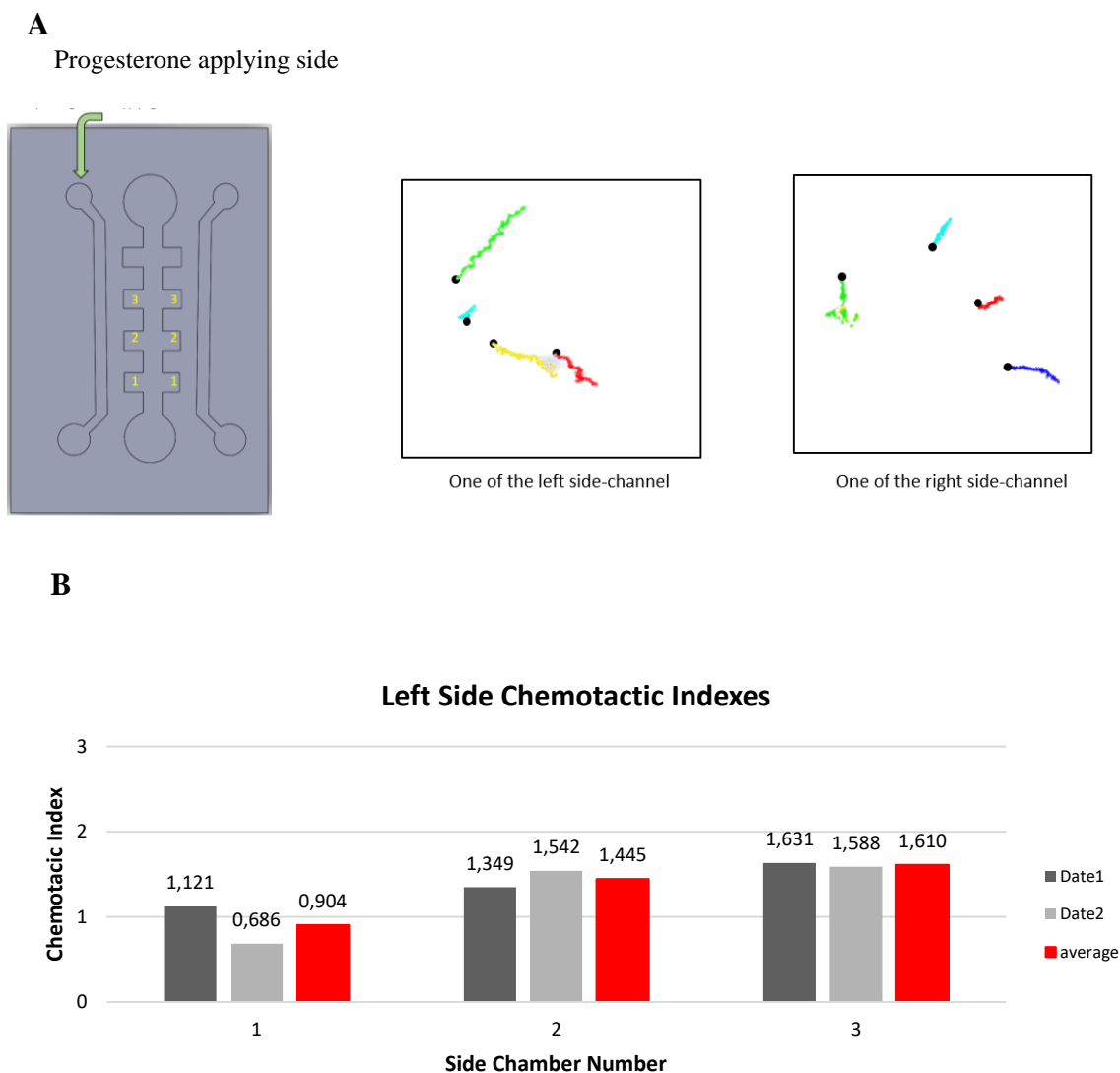


Figure 4.9: Spermatozoa trajectories (A) and indexes (B) when progesterone was applied from left side. Black dots show the final position of the spermatozoa movement. The numbers on the microfluidic device sketch (A) show the observed side-chambers and the bar under the sketch is the representative of progesterone gradient. Gray bars show the different dates which experiments were done as well as the red bars show the average chemotactic indexes.

When progesterone was applied from the left side-chamber, in theory spermatozoa must move towards that side. It can be seen from the trajectories (Figure 4.9-A), sperm cells move towards progesterone, even though the right side-chamber is far away from progesterone source. In terms of chemotactic indexes, mostly they are above 1 which means the number of the sperm cells is higher on the progesterone applied side (Figure 4.9-B). For the first side chamber, values

are below 1. When the sperm solution was inserted into the middle channel, it may affect the progesterone gradient in the channel. Therefore, the decrease in the indexes can be explained with that effect.

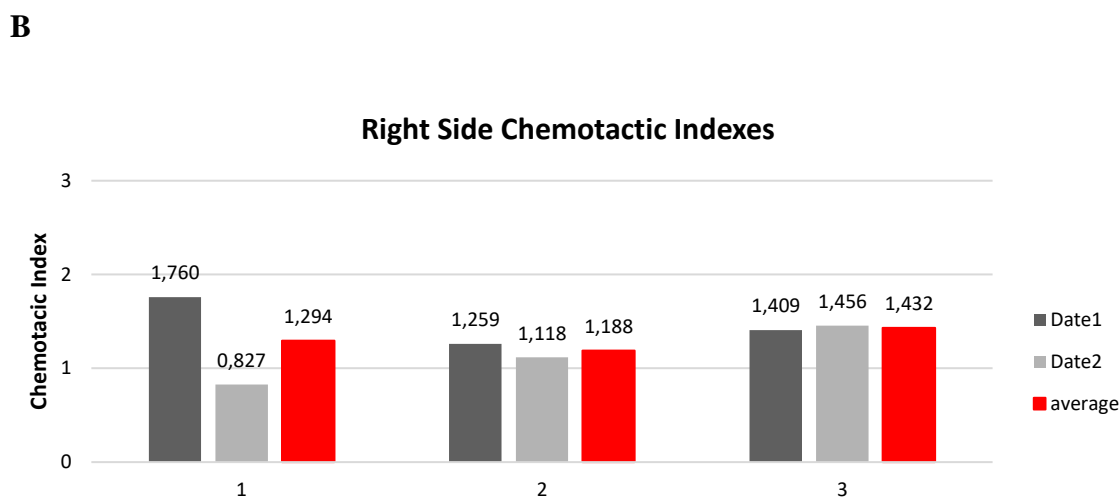
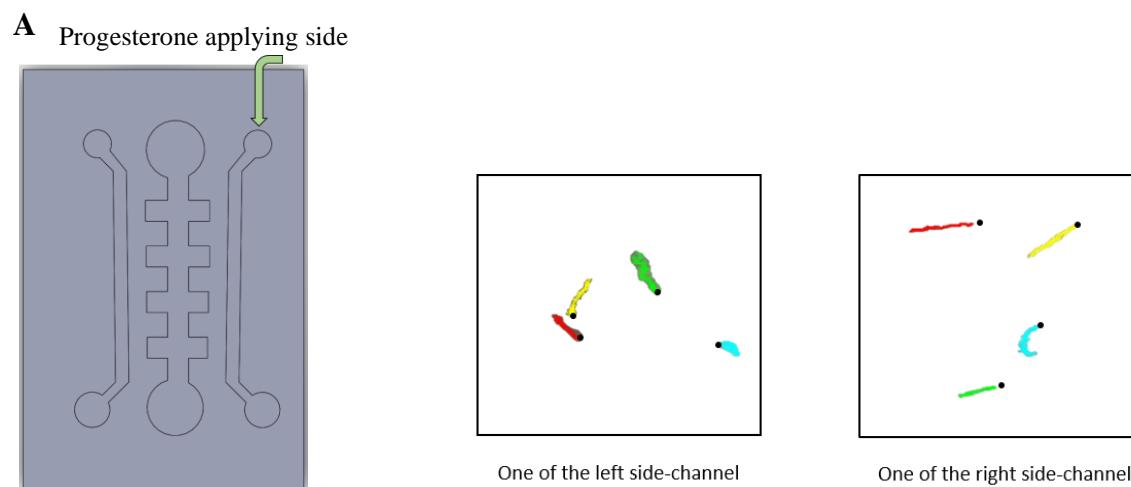


Figure 4.10: Spermatozoa trajectories (A) and indexes (B) when progesterone was applied from right side. Black dots show the final position of the spermatozoa movement. The numbers on the microfluidic device sketch (A) show the observed side-chambers and the bar under the sketch is the representative of progesterone gradient. Gray bars show the different dates which experiments were done as well as the red bars show the average chemotactic indexes.

Spermatozoa’s behavior towards chemoattractant gradient can be seen from Figure 4.10-A. There is a difference for the first side-chamber between two experiment dates (Figure 4.10-

B). This can be an experimental error. Nevertheless, the average values are above 1 and trajectories show that sperm cells move towards to progesterone gradient.

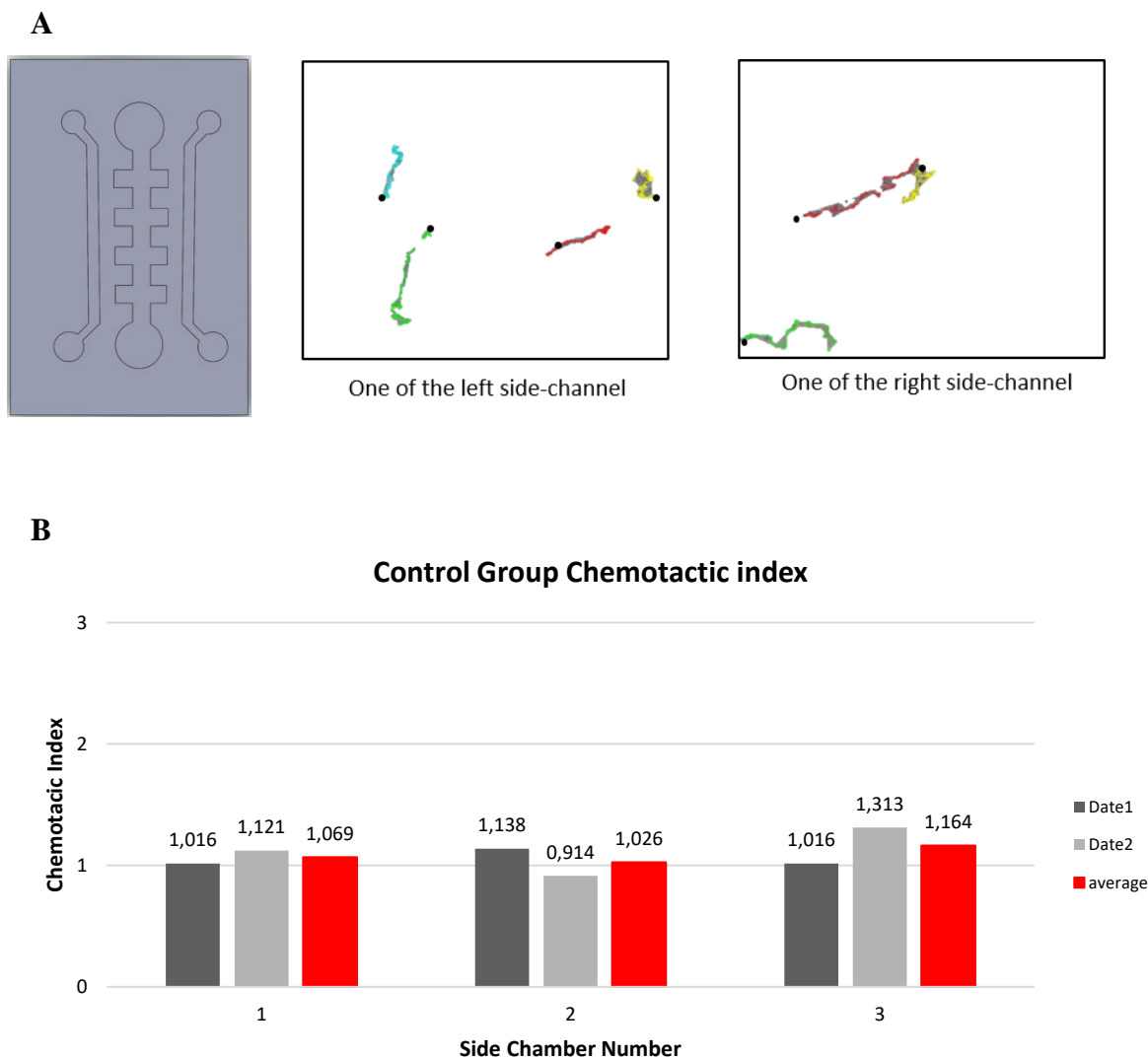


Figure 4.11: Spermatozoa trajectories (A) and indexes (B) for control group. Black dots show the final position of the spermatozoa movement. Gray bars show the different dates which experiments were done as well as the red bars show the average chemotactic indexes.

For the control group, all channels were empty at the beginning and then sperm solution was added into the middle channel. Since there was no chemoattractant effect, spermatozoa were moving around freely and even turning around themselves (Figure 4.11-A). The calculated indexes are nearly around 1. Some of them are below or above 1, but still they can be miscalculated because of ImageJ's cell counter plugin or can be experimental errors.

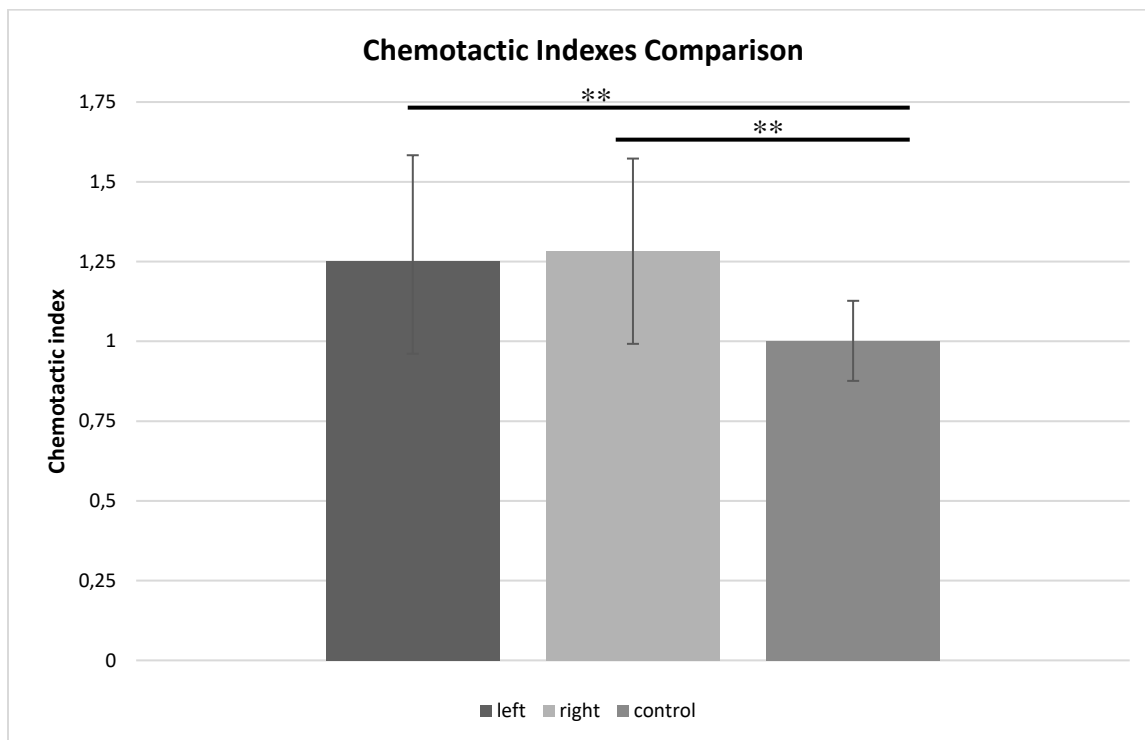


Figure 4.12: Comparison of the two different progesterone applying side with the control group which all the channels were empty. Indexes were calculated from 6 different observation areas. Data are presented as Mean \pm SD. **: $p < 0,05$.

In comparison of two different application sides of the chips and the control group, there is a significant difference (p : 0,0139 for progesterone was applied from right, as well as p : 0,0472 for the chips where progesterone applied from left side). When the two different applying sides were compared, there was not statistically different (p : 0,957). As a result, progesterone can be inserted into either left side-channel or right (Figure 22).

Xie L. et al. was performed a chemotaxis research and their calculated 'chemotaxis index' was between 0,75 and 1,25 [4] as well as our chemotaxis indexes was around 1,25 (Figure 4.12). Results from our study are in accordance with their study.

5. CONCLUSION AND OUTLOOK

Design from the previous study was used and hydrogel-based microfluidic device was fabricated with that design. Hydrogel solution concentration and fabrication method was optimized. Afterwards, viability test was performed to calculate live/dead ratio. Results showed that gelatin was the best to keep spermatozoa alive, however, due to its low melting point gelatin/agarose mixture was chosen for further experiments. Diffusion time was optimized to form proper gradient in the middle channel where the spermatozoa was injected and observed. With optimized gradient formation time, chemotaxis experiments were performed. 1 μM concentration of progesterone was used as a chemoattractant. To express the chemotactic behavior, 'chemotactic ratio' was calculated and results showed that sperm cells have a chemotaxis behavior. When the progesterone applying side was changed, there was no significant difference ($p: 0,957$), but difference between the control group and progesterone was significant.

Additionally, 2 μM concentration of progesterone was tried. However, results showed that spermatozoa died as soon as they enter the middle channel before start to move to the side-channels, as Zhang et.al (2015) reported [45].

It has been stated that progesterone is one of the known chemoattractant to the sperm cells [52]. Consequently, it can be said that spermatozoa may have a chemotaxis behavior.

6. LIST OF FIGURES

Figure 1.1: Potential improvements in the drug development pipeline as a result of the deployment of organ-on-a-chip and body-on-a-chip technologies into pharmaceutical research and development	2
Figure 1.2: Chemotaxis movement in female genital tract (A) and schematic of this behavior towards gradient (B)	4
Figure 3.1: Photograph of general structures of Nikon TE2000-U microscope.....	10
Figure 3.2: Illustration of heating plate and the temperature distribution	11
Figure 3.3: Design of the microfluidic device. Microfluidic chip has 3 channels (one middle channel and 2 side-channels) and 6 inlets/outlets	14
Figure 3.4: General steps of hydrogel solution preparation.	15
Figure 3.5: Chemical structure of (3-Aminopropyl)triethoxysilane (APTES) and glutaraldehyde (A).	16
Figure 3.6: The schematic of the cell viability assay general steps.....	17
Figure 3.7: Fluorescein solution was injected to one of the side channels and the area between side channel and middle channel, and the middle side of two side-chambers were observed with fluorescence microscopy.	19
Figure 3.8: Sketch of calculation of the chemotaxis ratio.	21
Figure 3.9: 3 different experiment groups to observe spermatozoa’s chemotaxis behavior.	22
Figure 4.1: Viability results of hydrogel-based microfluidic device which was made from agarose.	25
Figure 4.2: Viability results of hydrogel-based microfluidic device which was made from gelatin.....	27
Figure 4.3: Viability results of hydrogel-based microfluidic device which was made from gelatin/agarose mixture.	28
Figure 4.4: Comparison of three different hydrogel solutions’ viability rate within 20 minutes.	29
Figure 4.5: Agarose and gelatin/agarose gradient formation time experiment with sodium salt fluorescein solution.	31

Figure 4.6: Comparison of average intensity for the agarose and gelatin/agarose chips for the area that between middle channel and side channel 32

Figure 4.7: Agarose and gelatin/agarose gradient formation time experiment with sodium salt fluorescein solution. 33

Figure 4.8: Comparison of average intensity for agarose-based and gelatin/agarose-based chips for the middle channel. 34

Figure 4.9: Spermatozoa trajectories (A) and indexes (B) when progesterone was applied from left side. 36

Figure 4.10: Spermatozoa trajectories (A) and indexes (B) when progesterone was applied from right side. 37

Figure 4.11: Spermatozoa trajectories (A) and indexes (B) for control group. 38

Figure 4.12: Comparison of the two different progesterone applying side with the control group which all the channels were empty. 39

7. APPENDIX

List of abbreviations

PDMS polydimethylsiloxane

deionized (DI) water

3-Aminopropyl)triethoxysilane (APTES)

PBS Phosphate-buffered saline

polymethylmethacrylate (PMMA)

extracellular matrix (ECM)

fluorescein isothiocyanate (FTIC)

8. REFERENCES

- [1] S. Damiani, U.B. Kompella, S.A. Damiani, R. Kodzius, *Microfluidic Devices for Drug Delivery Systems and Drug Screening*, *Genes (Basel)* 9(2) (2018).
- [2] S.K. Bhupinder Singh Sekhon, *Microfluidics Technology for Drug Discovery and Development - An Overview*, *International Journal of PharmTech Research* 2(1) (2010) 804-809.
- [3] S. Koyama, D. Amarie, H.A. Soini, M.V. Novotny, S.C. Jacobson, *Chemotaxis assays of mouse sperm on microfluidic devices*, *Anal Chem* 78(10) (2006) 3354-9.
- [4] L. Xie, R. Ma, C. Han, K. Su, Q. Zhang, T. Qiu, L. Wang, G. Huang, J. Qiao, J. Wang, J. Cheng, *Integration of sperm motility and chemotaxis screening with a microchannel-based device*, *Clin Chem* 56(8) (2010) 1270-8.
- [5] L. Kang, B.G. Chung, R. Langer, A. Khademhosseini, *Microfluidics for drug discovery and development: from target selection to product lifecycle management*, *Drug Discov Today* 13(1-2) (2008) 1-13.
- [6] N. Khalid, S. Arif, I. Kobayashi, M. Nakajima, *Lab-on-a-chip techniques for high-throughput proteomics and drug discovery*, *Microfluidics for Pharmaceutical Applications 2019*, pp. 371-422.
- [7] A.G.G. Toh, Z.P. Wang, C. Yang, N.-T. Nguyen, *Engineering microfluidic concentration gradient generators for biological applications*, *Microfluidics and Nanofluidics* 16(1-2) (2013) 1-18.
- [8] J. Li, F. Lin, *Microfluidic devices for studying chemotaxis and electrotaxis*, *Trends Cell Biol* 21(8) (2011) 489-97.
- [9] D.T.C. Stephan K.W. Dertinger, Noo Li Jeon, George M. Whitesides, *Generation of Gradients Having Complex Shapes Using Microfluidic Networks*, *analytical chemistry* 73 (2001) 1240-1246.
- [10] A.D. Luster, R. Alon, U.H. von Andrian, *Immune cell migration in inflammation: present and future therapeutic targets*, *Nat Immunol* 6(12) (2005) 1182-90.
- [11] H. Chang, B.J. Kim, Y.S. Kim, S.S. Suarez, M. Wu, *Different migration patterns of sea urchin and mouse sperm revealed by a microfluidic chemotaxis device*, *PLoS One* 8(4) (2013) e60587.
- [12] E.T. Roussos, J.S. Condeelis, A. Patsialou, *Chemotaxis in cancer*, *Nat Rev Cancer* 11(8) (2011) 573-87.
- [13] R. Snyderman, L.C. Altman, M.S. Hausman, S.E. Mergenhagen, *Human mononuclear leukocyte chemotaxis: a quantitative assay for humoral and cellular chemotactic factors*, *J Immunol* 108(3) (1972) 857-60.
- [14] J.B. Pittenger, C.H. Dent, *A mechanism for the direct perception of change: the example of bacterial chemotaxis*, *Perception* 17(1) (1988) 119-33.
- [15] M. Eisenbach, *Bacterial Chemotaxis*, eLS2011.
- [16] O. Margie, C. Palmer, I. Chin-Sang, *C. elegans chemotaxis assay*, *J Vis Exp* (74) (2013) e50069.
- [17] A.E. Postlethwaite, A.H. Kang, *Collagen-and collagen peptide-induced chemotaxis of human blood monocytes*, *J Exp Med* 143(6) (1976) 1299-307.
- [18] S. Boyden, *The Chemotactic Effect of Mixtures of Antibody and Antigen on Polymorphonuclear Leucocytes*, (1961) 453-466.

- [19] P.G.Q. Robert D. Nelson, Richard L. Simmons, Chemotaxis Under Agarose: A New and Simple Method for Measuring Chemotaxis and Spontaneous Migration of Human Polymorphonuclear Leukocytes and Monocytes, *The Journal of Immunology* 115(6) (1975) 1650-1656.
- [20] M.J.H. Ko Y.J., Lee B.C., Lee S., Hwang S.Y., Ahn Y., <Separation of Progressive Motile Sperm from Mouse Semen Using on-ship Chemotaxis.pdf>, (2012).
- [21] M. Eisenbach, L.C. Giojalas, Sperm guidance in mammals - an unpaved road to the egg, *Nat Rev Mol Cell Biol* 7(4) (2006) 276-85.
- [22] R.L. Miller, Chemotaxis during fertilization in the hydroid *Campanularia*, *J Exp Zool* 162(1) (1966) 23-44.
- [23] D. Ralt, M. Manor, A. Cohen-Dayag, I. Tur-Kaspa, I. Ben-Shlomo, A. Makler, I. Yuli, J. Dor, S. Blumberg, S. Mashiach, et al., Chemotaxis and chemokinesis of human spermatozoa to follicular factors, *Biol Reprod* 50(4) (1994) 774-85.
- [24] F. Sun, L.C. Giojalas, R.A. Rovasio, I. Tur-Kaspa, R. Sanchez, M. Eisenbach, Lack of species-specificity in mammalian sperm chemotaxis, *Dev Biol* 255(2) (2003) 423-7.
- [25] J.J. Parrish, A. Krogenaes, J.L. Susko-Parrish, Effect of bovine sperm separation by either swim-up or Percoll method on success of in vitro fertilization and early embryonic development, *Theriogenology* 44(6) (1995) 859-69.
- [26] D. Ralt, M. Goldenberg, P. Fetterolf, D. Thompson, J. Dor, S. Mashiach, D.L. Garbers, M. Eisenbach, Sperm attraction to a follicular factor(s) correlates with human egg fertilizability, *Proc Natl Acad Sci U S A* 88(7) (1991) 2840-4.
- [27] J. Kopecek, Hydrogel biomaterials: a smart future?, *Biomaterials* 28(34) (2007) 5185-92.
- [28] B. Amsden, Solute Diffusion within Hydrogels. Mechanisms and Models, *Macromolecules* 31 (1998) 8382-8295.
- [29] A.D. Augst, H.J. Kong, D.J. Mooney, Alginate hydrogels as biomaterials, *Macromol Biosci* 6(8) (2006) 623-33.
- [30] N. Kashyap, N. Kumar, M.N.V.R. Kumar, Hydrogels for Pharmaceutical and Biomedical Applications, *Critical Reviews in Therapeutic Drug Carrier Systems* 22(2) (2005) 107-150.
- [31] B. Amsden, Solute diffusion in hydrogels. An examination of the retardation effect, *Polymer Gels and Networks* 6 (1998) 13-43.
- [32] S.P. Zustiak, H. Boukari, J.B. Leach, Solute diffusion and interactions in cross-linked poly(ethylene glycol) hydrogels studied by Fluorescence Correlation Spectroscopy, *Soft Matter* 6(15) (2010).
- [33] J. Fan, S. Li, Z. Wu, Z. Chen, Diffusion and mixing in microfluidic devices, *Microfluidics for Pharmaceutical Applications* 2019, pp. 79-100.
- [34] C.T.R. Nikolaos A. Peppas, Solute Diffusion in Swollen Membranes. Part I. A New Theory, *Journal of Membrane Science* 15 (1983) 275-287.
- [35] O.S. Yin, I. Ahmad, M.C.I.M. Amin, Synthesis of chemical cross-linked gelatin hydrogel reinforced with cellulose nanocrystals (CNC), 2014, pp. 375-380.
- [36] L.H.Y. Naziha Chirani, Lukas Gritsch, Federico Leonardo Motta, Soumia Chirani, Silvia Faré, History and Applications of Hydrogels, *Journal of Biomedical Sciences* 4 (2015).
- [37] S. Chen, Q. Zhang, T. Nakamoto, N. Kawazoe, G. Chen, Gelatin Scaffolds with Controlled Pore Structure and Mechanical Property for Cartilage Tissue Engineering, *Tissue Eng Part C Methods* 22(3) (2016) 189-98.

- [38] E. Varoni, M. Tschon, B. Palazzo, P. Nitti, L. Martini, L. Rimondini, Agarose gel as biomaterial or scaffold for implantation surgery: characterization, histological and histomorphometric study on soft tissue response, *Connect Tissue Res* 53(6) (2012) 548-54.
- [39] R. Imani, S.H. Emami, P.R. Moshtagh, N. Baheiraei, A.M. Sharifi, Preparation and Characterization of Agarose-Gelatin Blend Hydrogels as a Cell Encapsulation Matrix: An In-Vitro Study, *Journal of Macromolecular Science, Part B* 51(8) (2012) 1606-1616.
- [40] V. Verma, P. Verma, S. Kar, P. Ray, A.R. Ray, Fabrication of agar-gelatin hybrid scaffolds using a novel entrapment method for in vitro tissue engineering applications, *Biotechnol Bioeng* 96(2) (2007) 392-400.
- [41] S. Jovic, G. Mestres, M. Tenje, Fabrication of user-friendly and biomimetic 1,1'-carbonyldiimidazole cross-linked gelatin/agar microfluidic devices, *Mater Sci Eng C Mater Biol Appl* 76 (2017) 1175-1180.
- [42] Y. Qiu, B. Ahn, Y. Sakurai, C. Hansen, R. Tran, P.N. Mimche, R. Mannino, J.C. Ciciliano, T.J. Lamb, C.H. Joiner, S.F. Ofori-Acquah, W.A. Lam, Microvasculature-on-a-chip for the long-term study of endothelial barrier dysfunction and microvascular obstruction in disease, *Nat Biomed Eng* 2 (2018) 453-463.
- [43] A. Al-Abboodi, R. Tjeung, P.M. Doran, L.Y. Yeo, J. Friend, P.P. Yik Chan, In situ generation of tunable porosity gradients in hydrogel-based scaffolds for microfluidic cell culture, *Adv Healthc Mater* 3(10) (2014) 1655-70.
- [44] Seymour, <Seymour_et_al-2008-Limnology_and_Oceanography__Methods.pdf>, (2008).
- [45] Y. Zhang, R.R. Xiao, T. Yin, W. Zou, Y. Tang, J. Ding, J. Yang, Generation of Gradients on a Microfluidic Device: Toward a High-Throughput Investigation of Spermatozoa Chemotaxis, *PLoS One* 10(11) (2015) e0142555.
- [46] Y.H. Hussain, J.S. Guasto, R.K. Zimmer, R. Stocker, J.A. Riffell, Sperm chemotaxis promotes individual fertilization success in sea urchins, *J Exp Biol* 219(Pt 10) (2016) 1458-66.
- [47] R.R. Mather, *Synthetic Textile Fibres, Textiles and Fashion2015*, pp. 115-138.
- [48] S. Vira, E. Mekhedov, G. Humphrey, P.S. Blank, Fluorescent-labeled antibodies: Balancing functionality and degree of labeling, *Anal Biochem* 402(2) (2010) 146-50.
- [49] *Inverted_microscope_nikon_manual*.
- [50] <https://www.tokaihit.com/about-thermo-plate/>.
- [51] S.C.J. Christopher T. Culbertson, J. Michael Ramsey, Diffusion Coefficient Measurements in Microfluidic Devices, *Talanta* 56(365-373) (2002).
- [52] R. Oren-Benaroya, R. Orvieto, A. Gakamsky, M. Pinchasov, M. Eisenbach, The sperm chemoattractant secreted from human cumulus cells is progesterone, *Hum Reprod* 23(10) (2008) 2339-45.